Extremal black rings and hidden conformal symmetry

By

Dumisani Nxumalo

Submitted in partial fulfilment of the requirements for the degree

Masters of Science

In the

Department of Physics

Faculty of Agriculture and Natural Science

University of Pretoria

28 October 2019

Declaration

I Dumisani Nxumalo, declare that the dissertation, which I hereby submit for the degree, Masters in Science, at the University of Pretoria, is my own work and has not been previously been submitted by me for a degree at this or any other tertiary institutions.

____

(Dumisani Nxumalo)

____________________day of ____________________ 2019 in Pretoria, South Africa.

This dissertation is dedicated to my parents,
Linda and Busisiwe Nxumalo
who instilled in me the love of learning.

Acknowledgements

This work would not have been possible without the support and funding from the National Institute of Theoretical Physics.

I am also grateful for the support and guidance from my supervisor Professor K Zoubos. Without his patience and understanding, this work might not have reached completion. Furthermore, I am grateful for the support and financial assistance from my family and friends, who stood by side throughout the past two years. This is much their dissertation as it is mine.

Abstract

The goal of this master's research has been to ascertain whether Kerr/CFT correspondence techniques can be applied to black rings to better understand their CFT duals. Our efforts were largely focused on the hidden conformal symmetry of the Kerr black hole and how this approach can be applied and matched to black ring solutions. To this end, we show that the Kerr black hole hidden conformal symmetry technique for extremal black holes can be applied to a $U(1)^3$ supersymmetric black ring and the extremal double rotating black ring solutions. This allows us to determine the microscopic temperature of the left moving sector. To confirm our result, we compare our computation for the microscopic entropy (using the Cardy formula) to those obtained either through Bekenstein-Hawking formula or the asymptotic symmetry group approach.

Contents

List of Figures

1

Introduction

1.1 General Relativity : An overview

General relativity is arguably one of the most successful theories of modern theoretical physics. Its predictions have been confirmed by numerous astrophysical observations. One of its most fundamental predictions is the existence of gravitational singularities. These singularities are often referred to as black holes and can be loosely defined as a region of spacetime where a solution to Einstein field equations approaches infinity. Black holes have been observed in our universe as we experience it, and this makes them interesting to study from a theoretical perspective.

The first black hole solution to Einstein's equations was constructed by Karl Schwarzschild in 1916. The solution represents a spherically symmetric geometry of empty spacetime outside a massive object [1]. The Schwarzschild metric is:

$$ds^2 = -\Big(1 - \frac{2Gm}{r}\Big)dt^2 + \Big(1 - \frac{2Gm}{r}\Big)^{-1} dr^2 + r^2(d\theta^2 + \sin^2\theta d\phi^2). \tag{1.1}$$

Where m is the mass of the black hole. The event horizon is located at $r = 2m$ [2, 3, 1]. G is the Newton gravitational constant. At $r = 0$ and $r = 2Gm$ we have a singularity. The singularity at $r = 2Gm$ is coordinate dependent and can be done away with an appropriate change in coordinates. The event horizon in the context of black holes is a region of spacetime beyond which light cannot escape as a result of the mass of the black hole.

Following the Schwarzschild solution there was another black hole solution to Einstein's field equations put forward by Hans Reissner, Gunnar Nordstrom (Reissner-Nordstrom). Reissner published his paper in 1916 and Nordstrom two years later, in 1918. Their solution is a representation of spacetime outside a spherically symmetric charged body with electric charge. This body however, does not have spin or a magnetic dipole [1, 4, 5].

Almost half a century later, in 1963, Roy Kerr constructed another black hole solution to Einstein's field equations. Unlike the Schwarzschild solution which is premised on a static coordinate system and predicted the existence of a static black hole, the Kerr solution is premised on a rotating (but stationary) coordinate system, resulting in the prediction of a rotating black hole. The Kerr geometry and black hole forms the backbone of our research and will be discussed in more detail in the next chapter. What makes the Kerr solution (and the Schwarzschild one) particularly interesting to study, is that their existence has been confirmed through astrophysical and cosmological observations[6].

It took almost another 20 years (1986) for another black hole solution to Einstein's field equations to be constructed. This time it was by the duo, Malcolm Perry and Robert Myers. Unlike Schwarzschild's and Kerr's solution, their solution did not "live" in the 4 dimensions of spacetime, it existed in $d \geq 5$ dimensions. Their solutions came after theories like String theory, Super-Symmetry (SUSY) and Super-gravity (SUGRA) had been studied for years. These theories have largely been studied in higher dimensional spacetime. Following the discovery of their 5D black hole solution the authors of [7] conjectured the existence of non-spherical black objects. One of the predicted non-spherical objects is a black ring, a black object with $S^1 \times S^2$ topology.

Fortunately we did not have to wait too long for a non-spherical black hole solution to Einstein's equations to be constructed. The first black ring solution was constructed in 2001 by Roberto Emparan et al [8]. In 2003 the first super-symmetric black ring solution was constructed, and since then there has been numerous black ring solutions constructed, both super-symmetric and non-super-symmetric [9]. As this work is dedicated to the application of the Kerr/CFT correspondence to black ring solutions, we also dedicated a chapter to the review of black ring solutions (chapter 3).

As one can infer from the sporadic discovery of exact black hole solutions to Einstein's equations, the differential equations making up Einstein's field equations are far from trivial. However this is not the only challenge associated with general relativity. One of the long standing unresolved problems in high energy theoretical physics is how general relativity can be reconciled with quantum mechanics. Both general relativity and quantum field theory have proven extremely successful theories independently, however, general relativity breaks down at the "quantum" scale. We will park the discussion on the lack of congruence between general relativity and quantum mechanics and return to it in section 1.3. We will now look at general relativity in higher dimensions.

1.2 General Relativity in Higher Dimensions

As we have seen, general relativity at higher dimensions presents a number of interesting theoretical phenomena. We've already touched on one of these phenomena in the context of black objects, i.e. the black ring. A natural question one might ask, is whether the physics in $d > 4$ is different from the physics in our "normal" $d = 4$ dimensions of spacetime? The answer to this question is a resounding yes. One of the reasons for this difference is attributed to the fact that, as one increases the number of dimensions, the number of degrees of freedom of the gravitational field also increase [10].

One can see why there would be a significant difference between physics in $d = 4$ dimensions and $d \geq 5$ by studying two aspects of rotation. Firstly, there is a possibility of rotation in several independent planes. Secondly, in higher dimensions, one expects that there would be competition between gravitation and centrifugal potentials. The radial fall off of the Newtonian potential is of the order of GM/r^{d-3} and that of the centrifugal barrier, J^2/M^2r^2. As can be seen, the gravitational potential depends on the number of dimensions, whereas the centrifugal potential does not [10].

Another interesting phenomenon that we see in $d \geq 5$ dimension physics, not seen in $d = 4$ dimensions, is the appearance of black objects with extended topologies. We've already touched on black rings but we have not mentioned black strings and black p-branes. These do not provide us with asymptotically flat solutions, however they do provide us with a way of understanding novel kinds of asymptotically flat black holes [10].

One can see how it is possible to have non-spherical black objects in $d \geq 5$ dimensions by considering a black hole in d dimensions with a particular horizon geometry, say for example, Σ_H geometry. We can construct a vacuum solution in $d + 1$ dimensions by adding a flat spatial direction. The new horizon would then be a black string with horizon $\Sigma_H \times \mathbb{R}$. The Schwarzschild solution has been generalised to $d \geq 4$ dimensions, and it can be argued that black strings exist in $d \geq 5$. Given that the string has tension, we can imagine this string being curved into a ring, then we would have a black ring. Since the string is contractable and will tend to collapse, if we have the ring rotating, we would then have a centrifugal force (providing repulsion) balancing the tension of the string. This requirement of rotation implies that we cannot have static black rings. On the other hand, if we add p flat directions, instead of adding a single flat direction, we then find black p-branes with horizon $S^q \times \mathbb{R}^p$ with $q \geq 2$. These exist in any $d \geq 6 + p - q$ dimensions [10].

In the next section we briefly discuss the "information paradox" associated with black holes. The information loss paradox is one of the long standing problems associated with black holes and general relativity. We also provide a high level overview of quantum theories of quantum gravity, which seek to solve this problem amongst others.

1.3 Quantum Theories of Gravity

One of the most long standing problems in theoretical physics is the black hole information paradox. Any theory of quantum gravity should resolve this problem if it is to prove useful. There are various ways the paradox manifests itself. We will briefly state three of these.

1.3.1 Information Paradox

One of the ways the information paradox comes about is as a result of the quantum mechanical evolution of black holes. This has been observed in black holes which form as a result of a non-singular initial data point, for example black holes forming as a result of stellar collapse. Such black holes emit particles as hot bodies and have been shown to eventually evaporate as a consequence of Hawking radiation [11, 12, 13]. At the beginning of the collapse, the in falling matter around the black hole is in a pure a quantum state. From the Hawking radiation we have a thermal state, as a result we end up with an evolution from a pure quantum state (of the in falling matter) to a mixed state (both quantum and thermal). This is an example of the violation of the quantum unitary principle. The quantum unitary principle is statement to the effect that the number of states at the beginning of any quantum process should be the same as the number of states at the end of the process [12].

Another way the information paradox manifests itself is through excitations on the background of extremal black holes which are a pure quantum state. The resulting non-extremal black hole will emit Hawking radiation until it approaches extremality, thus moving from a mixed state to a pure quantum state. An extremal black hole can be thought of (in the context of the Reissner-Nordstrom black hole) as a black hole with $GM^2 = p^2 + q^2$ where G is the Newtonian gravitational constant, M the mass, p is the total magnetic charge and q is the total electric charge with the black hole.

The third way the information paradox manifest itself can be described as follows; if we consider an equilibrium state where energy is put into the black hole at the same rate as it is evaporating. The information paradox arises from the fact that an arbitrary amount of information can be encoded into the energy that is put into the black hole over time. This energy can be of different forms and most of this information is lost and cannot be recovered through Hawking radiation [12].

Viewing black holes as quantum states, one is naturally led to ask the question of whether there are signs of the classical singularity in the final quantum description of black holes [14]. This leads us to a discussion on the leading theories of quantum gravity.

1.3.2 Candidate Theories

There are several approaches towards the quantum theory of gravity, even though all these theories are essentially trying to resolve the same problem. As one can expect, they differ primarily on the assumptions they make. We will not discuss all of them here, we will focus on only two "leading" candidate theories; these being string theory and loop quantum gravity.

1.3.2.1 String Theory

The most prominent of the theories of quantum gravity has been string theory. This theory has been studied since the 1970s and initially held great promise as a quantum theory of gravity. The theory was initially studied in the context of quantum chromodynamics (QCD), specifically to better understand strong interactions. Mesons in this framework can be thought of as open strings, with a quark at one end (of the string) and an anti-quark at the other end [15].

String theory rests on the assumption that the most fundamental building block of nature is a string, a one dimensional extended object [13]. This string lives in $d = 26$ dimensions for the bosonic string and $d = 10$ dimensions for the superstring. In our "normal" $d = 4$ dimensions of spacetime the string is conjured to be coiled and manifesting itself as particles. Gravity in string theory is seen as just one of the excitations of the string living in some background metric [16, 17].

Given its formulation, string theory has proved difficult to test through experiments and observations. However is has proved very useful in other areas. An area which has been studied a great deal recently has been the AdS/CFT correspondence whose subset, the Kerr/CFT correspondence, is the subject of this dissertation. Although it has been demonstrated numerous times [18, 19] that one does not have to assume the validity of string theory or even SUSY for AdS/CFT to produce meaningful results; the derivation of AdS/CFT is nonetheless based on the assumption that both string theory and SUSY are valid [20, 13, 21]. We provide a high level overview of AdS/CFT in section 1.5.

1.3.2.2 Loop Quantum Gravity

Loop quantum gravity, on the other hand, can be summarised as an attempt to quantise general relativity. By definition it assumes the correctness of both quantum mechanics and general relativity. And, as we stated earlier, both quantum field theory (a generalisation of quantum mechanics) and general relativity have been proven successful in experiments and observations.

The approach of loop quantum gravity can be stated as follows; assume there is no background in space, reconstruct quantum field theory in a form that does not require background space. The basis of loop quantum gravity is the idea that the natural variables describing a Yang-Mills field theory are Faraday's "lines of force". A Faraday line of force can be thought of as an elementary quantum excitation of the field. In the absence of charges these lines must close themselves to form loops. Loop quantum gravity (LQG) is the mathematical description of a quantum gravitational field in terms of these loops. The loops in LQG are thought of as quantum excitations of the Faraday lines of force of the gravitational field [22].

To close-off this brief digression into the quantum theory of gravity, we would like to point out two the key differences between string theory and loop quantum gravity. We have already alluded to the first one, i.e. LQG, like general relativity is not background dependent whereas string theory is. Secondly, LQG does not attempt to unify all four fundamental forces of physics, whereas string theory does make this attempt [23, 22, 14]. In the next section we briefly discuss the thermodynamics of black holes as this provides the foundation for our discussion of entropy later in the report.

1.4 Black holes and thermodynamics

There is an amazing resemblance between the laws of thermodynamics and those of black hole mechanics [24]. To illustrate this resemblance, we start by looking at the zeroth law of thermodynamics. It states that the temperature of a body at equilibrium is constant throughout the body. If not, it flows from regions of high temperature to those of low temperature. For black holes we have a quantity referred to as surface gravity, κ, which remains constant on the event horizon. This "conservation" principle for black holes is true for all black holes, for both spherically symmetric and non-spherical horizons of spinning black holes [2, 25]. It has been shown that the temperature of a black hole is related to the surface gravity. When quantum effects are taken into account, the temperature of a black hole is not zero but is $\kappa/2\pi$, this is after choosing natural units such that $\hbar = G = c = 1$. In this scenario a black hole can be observed to absorb and emit particles in the same way as a perfect black body at that temperature [2, 25].

The 1st law of thermodynamics states that in any process, energy is conserved, i.e. $dE = TdS + \mu dQ + \Omega dJ$, where T is the temperature, E is the energy, S is the in entropy, Q is the charge with chemical potential μ, and J is the spin with chemical potential Ω. The corresponding "law" for black holes is, $dM = \frac{\kappa}{8\pi G}dA + \mu dQ + \Omega dJ$. Where M is the mass of the black hole, A is the area of the black hole horizon.

Our main interest is in the 2nd law of thermodynamics and how it relates to the black holes. The 2nd law states that in any physical process the change in the total entropy always increases $\delta S \geq 0$, i.e. it never decreases. With regards to black holes, the area theorem states that the area of all black holes in the universe never decreases. We have $\delta A \geq 0$ related to the area of the event horizon of the black hole as conjectured in [2, 25]. The entropy of matter outside the black hole relates to the area of the event horizon of the black hole as [26, 27];

$$S_{entropy} = \frac{\mathcal{A}}{4G}, \tag{1.2}$$

Where $\mathcal{A}$ is the area of the event horizon and G is the Newton gravitational constant. This equation(1.2) will also appear when we confirm our result for the entropy in chapter 5.

1.5 AdS/CFT: High-level overview

In this section we will not go into the detail of the derivation of the AdS/CFT correspondence, we only provide a high level overview of what it is, its implications for quantum gravity and the study of black holes.

1.5.1 Anti de Sitter spacetime

Before we go into the detail of what exactly the AdS/CFT correspondence is, it will be useful for us to remind ourselves of the geometry of the anti de Sitter(AdS) spacetime. AdS is a spacetime of constant negative curvature ($R < 0$) [1], where R is the Ricci scalar. The metric of AdS spacetime is[1] [28, 21],

$$ds^2_{AdS_{d+1}} = L^2\Big[-(r^2+1)dt^2 + \frac{dr^2}{r^2+1} + r^2 d\Omega^2_{d-1}\Big]. \tag{1.3}$$

[1]By applying an appropriate change of coordinates, the metric (1.3) can also be expressed as $ds^2 = R^2(-\cosh^2\rho d\tau + d\rho^2 + \sinh^2\rho d\Omega^2)$, which is usually referred to as global coordinates for AdS.

The time direction, t, in the metric above (1.3) is compact and the last term is a unit sphere, S^{d-1} [28]. AdS space provides us with a geometric description of a hyperboloid [1]. The radius of curvature is L. Near $r = 0$, AdS space approximates flat space and moving towards larger values of r we see that the term in front of dt^2, g_{tt}, and the unit sphere grows larger. The growth of g_{tt} can be viewed as growth in gravitational potential. A slowly moving particle feels a gravitational potential $V \sim \sqrt{-g_{tt}}$. If it is at rest at large r, it will be in an oscillatory motion in the r direction, reminiscent of a particle in a harmonic oscillator [28]. The boundary has an $R \times SO(d)$ symmetry. The full symmetry group of the AdS space is $SO(2, d)$ [28, 21].

One of the properties which make AdS space quite useful is its isometries. One can think of isometries as maps from one metric space to another, which preserve the metric. The isometries of the embedding space of AdS in $d+1$ dimensions are the full symmetries of AdS in d dimensions. This isometry group $SO(2, d)(SO(2, d+1)$ in Euclidean signature) acts on the boundary as the conformal group [31].

1.5.2 Conformal Field Theory(CFT)

A field theory has conformal symmetry if it is invariant under conformal transformations. A conformal transformation is a change of coordinates $\sigma^\alpha \rightarrow \bar{\sigma}^\alpha(\sigma)$ such that the metric transforms as,

$$g_{\alpha\beta}(\sigma) \rightarrow \Omega^2(\sigma) g_{\alpha\beta}(\sigma). \tag{1.4}$$

This translates to a theory that is the same at all length scales. Conformal theories care about angles, not distances [16].

A transformation of the form of (1.4) has different interpretation depending on whether the background is dynamical or fixed. When the background is dynamical, as in the Kerr black hole solution, the transformation is a diffeomorphism, and we have a gauge symmetry. When the background geometry is fixed, the transformation can be thought of as a physical symmetry taking a point $\sigma^\alpha \rightarrow \bar{\sigma}^\alpha$. We get a global symmetry with the corresponding conserved charge [16].

The conformal transformation is locally equivalent to (pseudo) rotation and dilation. The set of conformal transformations form a group, the conformal group [29]. The generators of the conformal group are provided in Appendix A. There is an isomorphism between the conformal group and the group $SO(d+1, 1)$ [29]. The algebra obeyed by these generators is also provided in appendix A. We will not go further into global conformal field theories, readers interested in a more detailed discussion and the development of ideas around conformal field theories can see [29, 17, 16].

1.5.3 AdS/CFT

The AdS/CFT correspondence or the gauge/gravity duality is a conjecture which states that all the physics in an asymptotically AdS spacetime can be described by a local quantum field theory that lives on its boundary [28, 30, 31, 21]. A slightly more involved (and technical) description of AdS/CFT is that the large N limit of a conformally invariant theory in d dimensions is governed by supergravity (and string theory) on $d+1$ AdS space [21]. This was the initial proposal by Maldacena in [20].

How this manifests itself is through the action of the isometries of AdS on the boundary. The boundary is given by $R \times S^{d-1}$. They (isometries) act on the boundary, they send points on the boundary to other points on the boundary. These isometries on the boundary provide a representation of the conformal group in d dimensions, $SO(2,d)$. A conformal field theory is a type of a quantum field theory. The boundary theory is scale invariant and does not have a "dimensionful" parameter [28]. Therefore AdS/CFT allows us to see a $d+1$ dimensional theory (a theory of gravity) in the bulk of AdS is equivalent to a d dimensional theory (a CFT) on the boundary [28].

The AdS/CFT correspondence is often referred to as the holographic principle. We have already hinted at this holography, however it can be demonstrated somewhat more clearly by looking at the Bekenstein bound. The Bekenstein bound states that the maximum entropy in a region of space is $S_{max} = Area/4G_N$, where G_N is the Newtonian gravitational constant. The area is that of the boundary region. Suppose we had a state with more entropy than S_{max}, then the 2nd law of thermodynamics will be violated. Furthermore, if more matter is thrown in, such that a black hole is formed, then the entropy cannot decrease. However if a black hole forms inside this region its entropy would then be proportional to area of the horizon, which is smaller than the initial entropy. This then would be a violation of the 2nd law of thermodynamics. The Bekenstein bound implies that the number of degrees of freedom inside some region grows as the area of the boundary (of the region) and not its volume. This is not consistent with quantum field theory. The attempt to try and understand this leads to the "holographic principle" which states that in a quantum theory of gravity, all physics within some volume can be described in terms of some theory on the boundary which has less than one degree of freedom per Planck area. This leads to the entropy satisfying the Bekenstein bound [13]. For an introductory discussion of AdS/CFT the reader can see [28], and for a more technical discussion and derivation of the conjecture, [20, 30, 31, 21].

AdS/CFT allows us to obtain non-perturbative information on ordinary, but mostly conformal invariant quantum field theories. This is especially true for those quantum theories in the large N limit (of the gauge group, $U(N)$). This non-purtabitive information is obtained from classical string/M-theory or classical supergravity [31]. The conjecture has proved quite useful in the study of black holes. It has allowed us to connect the entropy of a black hole with an ordinary thermal entropy of a field theory. This allows us to have a statistical interpretation of black hole entropy. It gives us the insight to see a black hole as an ordinary thermal state in a unitary quantum field theory. From this we are then able to see black holes as being consistent with quantum mechanics and the unitary evolution principle [28]. It also provides us with the tools to study free energy and other thermal states in quantum field theories, which have gravity duals.

In concluding this introductory chapter, we would like to point out (as of the time of writing) there is no mathematically rigorous proof of the AdS/CFT correspondence. It has proved very successful in producing results that have been confirmed through other approaches and through observation, however, we are yet to see a mathematically consistent proof of the conjecture. In the next chapter we motivate for the Kerr/CFT conjecture, a subset of AdS/CFT. We also review the derivation of the hidden conformal symmetry of the Kerr black hole solution.

2

Kerr/CFT Correspondence

The Kerr/CFT correspondence can be divided into two broad categories; the strong Kerr/CFT conjecture which is a statement about quantum gravity and relies on the asymptotic symmetry group in its derivation. The second category is the weak Kerr/CFT conjecture, which can be described as mapping conformal coordinates to the quadratic Casimir of the $SL(2,\mathbb{R})_L \times SL(2,\mathbb{R})_R$ group to find hidden conformal symmetries in the near region of the Kerr black hole.

What makes the Kerr/CFT correspondence particularly interesting to study is that unlike AdS/CFT which assumes the validity of String theory and assumes Super-Symmetry(SUSY), Kerr/CFT is an expression of a duality between general relativity and a 2D conformal field theory (CFT), without assuming either String theory or SUSY. In the first paper on Kerr/CFT by Strominger et al [6],the authors argued that extreme Kerr black holes are dual to a 2-d chiral CFT. This followed the work by Brown and Hennaux, who argued that AdS_3 spacetime is dual to a 2D conformal theory [18]. This was a significant result in a sense that both Schwarzchild and Kerr black holes have been observed in the sky and we could now link these entities to a quantum field theory.

2.1 Kerr/CFT a statement of quantum gravity

We start our review by looking at the strong Kerr/CFT conjecture. The key result of the Kerr/CFT correspondence was the computation of the central charge associated with near horizon extremal (NHEK) geometry of the Kerr black hole. The process of determining this central charge begins with defining the NHEK geometry.

2.1.1 Near Horizon Extremal Kerr

In order to arrive at the near horizon region of the extremal Kerr black hole, we firstly need to define what is meant by an extremal Kerr black hole. To arrive at the extreme Kerr geometry we use the Boyer-Lindquist coordinates in defining the metric of the Kerr black hole. The metric in these coordinates takes the form;

$$ds^2 = \frac{\rho^2}{\Delta}d\hat{r}^2 - \frac{\Delta}{\rho^2}(d\hat{t} - (J/M)\sin^2\theta d\hat{\phi})^2 + \rho^2 d\theta^2 + \frac{\sin^2\theta}{\rho^2}\Big((\hat{r}^2 + (J/M)^2)d\hat{\phi} - (J/M)^2 d\hat{t}\Big)^2 \quad (2.1)$$

where we have,

$$\Delta = \hat{r}^2 + (J/M)^2 - 2GM\hat{r}, \qquad \rho^2 = \hat{r}^2 + (J/M)^2 \cos^2\theta \tag{2.2}$$

M is the mass, and J is the angular momentum of the black hole. Unlike to the Schwarzschild black solution, the Kerr solution has two horizons, the inner and outer horizons. These follow from setting $\Delta = 0$ and are located at,

$$r_{\pm} = GM \pm \sqrt{G^2M^2 - (J/M)^2} \tag{2.3}$$

The extremal case of the Kerr black hole solution occurs when $GM^2 = J$, and it saturates the bound $J \leq GM^2$. If we have additional angular momentum at the same mass, i.e. $(J \geq GM^2)$, this results in a naked singularity which is a violation of the cosmic censorship conjecture [6].

We now need to work out a metric of the black hole very close to the event horizon. For the remainder of this discussion on the Kerr/CFT correspondence, the focus will be on the extremal limit of the Kerr black hole, i.e $J = GM^2$. To do this, we perform the following transformations and take the limit as $\lambda \to 0$.

$$t = \frac{\lambda\hat{t}}{2M}, \qquad y = \frac{\lambda M}{\hat{r} - M}, \qquad \phi = \hat{\phi} - \frac{\hat{t}}{2M}. \tag{2.4}$$

After taking the limit $\lambda \to 0$, keeping (t, y, ϕ, θ) fixed, the metric becomes,

$$ds^2 = 2GJ\Omega^2\Big(\frac{-dt^2 + dy^2}{y^2} + d\theta^2 + \Lambda^2\big(d\phi + \frac{dt}{y}\big)\Big)^2, \tag{2.5}$$

where,

$$\Omega^2 \equiv \frac{1 + \cos^2\theta}{2}, \qquad \Lambda \equiv \frac{2\sin\theta}{1 + \cos^2\theta}. \tag{2.6}$$

The angle θ takes on the values, $0 \geq \theta \geq \pi$, and $\phi \approx \phi + 2\phi$. The shift from $\hat{\phi}$ to ϕ makes $\frac{\partial}{\partial t}$ tagent to the horizon [32].

We perform the following coordinate transformation.

$$\begin{aligned} y &= \Big(\cos\tau\sqrt{1 + r^2} + r\Big)^{-1}, \\ t &= y\sin\tau\sqrt{1 + r^2}, \\ \phi &= \varphi + \ln\Big(\frac{\cos\tau + r\sin\tau}{1 + \sin\tau\sqrt{1 + r^2}}\Big). \end{aligned} \tag{2.7}$$

This transforms our metric (2.1) to the near horizon extremal Kerr(NHEK) geometry. The result is the NHEK geometry expressed in global coordinates. The metric takes the form of,

$$d\bar{s}^2 = 2GJ\Omega^2\Big(-(1 + r^2)d\tau^2 + \frac{dr^2}{1 + r^2} + d\theta^2 + \Lambda^2(d\varphi + rd\tau)^2\Big) \tag{2.8}$$

The above process of defining the NHEK geometry was initially put forward by Horowitz and Bardeen in [32]. The NHEK geometry has an $SL(2,\mathbb{R}) \times U(1)$ isometry group. The rotational $U(1)$ isometry is generated by the Killing vector [6],

$$\zeta_0 = \partial_\varphi. \tag{2.9}$$

Now that we have our NHEK metric (2.8), the next step is to determine boundary conditions which will enable us to identify diffeomorphism consistent with the symmetries of the asymptotic group of the NHEK background. The charges which generate these diffeomorphisms will ultimately lead to the expression for the central charge.

2.1.2 Boundary Conditions

Specifying boundary conditions which have the appropriate fall-off rates for metric perturbations is a key step in working out the asymptotic symmetry group. In identifying these boundary conditions Strominger et al in [6] were informed by the work of Brown and Henneaux in [18] where they were able to work out boundary conditions consistent with the asymptotic symmetry group of $3d$ Einstein gravity. With appropriate boundary conditions, one can then proceed to analyse asymptotic symmetries, which form a group consistent with the chosen boundary conditions. The asymptotic symmetry group can be thought of as a group of gauge symmetries whose parameters fall at a rate slow enough that they lead to a non-zero charge [33]. Conducting the asymptotic symmetry group analysis can be summarised as finding diffeomorphisms (vector fields ζ) whose action on the metric (Lie derivative $\mathcal{L}_\zeta g$) generates metric fluctuations consistent with the boundary conditions [34]

When the boundary conditions have been specified, we can then identify a set of diffeomorphism consistent with these boundary conditions. We can think of these diffeomorphism as vectors which preserve the boundary conditions. The diffeomorphisms then form an asymptotic group. The diffeomorphisms which preserve the boundary conditions associated with the NHEK geometry are form of [6, 35];

$$\xi = \left[-r\epsilon'(\varphi) + O(1) \right]\partial_r + \left[C + O(\frac{1}{r^3}) \right]\partial_\tau + \left[\epsilon(\varphi) + O(\frac{1}{r^2}) \right]\partial_\varphi + O(\frac{1}{r})\partial_\theta, \tag{2.10}$$

where $\epsilon(\varphi)$ is an arbitrary smooth function of the boundary coordinate φ. The C in the above expression is an arbitrary constant.

From the diffeomorphisms it has been shown that the asymptotic group of the NHEK geometry has a single copy of conformal group within it which is generated by,

$$\zeta_\epsilon = \epsilon\varphi\partial_\varphi - r\epsilon'(\varphi)\partial_r \tag{2.11}$$

A key element of these diffeomorphisms is the fact that they allow a single copy of the Virasoro algebra. This result followed the discovery that NHEK geometry contained a self-dual orbifold, and this self dual orbifold has been shown to contain a copy of the Virasoro algebra. For a brief discussion on this, the reader can see section 2.1.5.

2.1.3 Charges

The diffeomorphism discussed above obey a Lie bracket algebra. They are also generated by conserved charges. These charges adhere to the same boundary conditions associated with the symmetries of the asymptotic group. The ultimate objective of computing the charges which generate the diffeomorphism of the asymptotic group is to eventually arrive at a point where we can compute the central charge associated with the NHEK region. How this will be achieved will be to compute the symmetry algebra associated with the charges and see if there is a central extension(term). From the central extension we can then read off the central charge.

Firstly we observe that given a diffeomorphism ζ, consistent with the boundary conditions of the ASG, the generator of this diffeomorphism is a conserved charge $Q_\zeta[g]$ [35]. To proceed, we need to establish the infinitesimal differences between the charges which generate the diffeomorphism when the metric is perturbed such that it preserves the boundary conditions. The infinitesimal difference is computed between two close backgrounds, in the Kerr case, $g_{\mu\nu}$ and $g_{\mu\nu} + h_{\mu\nu}$. Where $h_{\mu\nu}$ is a small perturbation of the NHEK metric. The infinitesimal charge difference is expressed as an integral of the surface charge form, k_ζ, between two neighbouring geometries and the integral is taken over some spacial slice [35, 33]. The expression for the infinitesimal charge difference is,

$$\delta Q_\zeta[h,g] = \frac{1}{8\pi G}\int_{\partial\Sigma} k_\zeta[h,g] \tag{2.12}$$

The surface charge form, $k_\zeta[h,g]$, is a tensor which has its origins in the analysis of "gauge symmetries" within the boundaries of AdS spacetime. When we take the integral of the infinitesimal charge difference we then end up with the total charge.

$$Q_\zeta[h,g] = \int_\tau \int_{\partial\Sigma} k_\zeta[h,g], \tag{2.13}$$

where τ is the path in our background that takes us from $g_{\mu\nu}$ to $g_{\mu\nu}+h_{\mu\nu}$. This can only happen if the integrability condition is satisfied, i.e. the value of the total charge is independent of the path of integration [33, 36].

We now look at the charges that generate the ∂_τ and ζ_ϵ,

$$Q_{\partial_\tau} = \frac{1}{8\pi G}\int_{\partial\Sigma} k_{\partial_\tau} \qquad Q_{\zeta_\epsilon} = \frac{1}{8\pi G}\int_{\partial\Sigma} k_{\zeta_\epsilon} \tag{2.14}$$

With the charges we can then take the charge algebra, this is done by varying one charge with respect to the other diffeomorphism. Hence commutator of the charges takes the form [33, 36],

$$\{Q_{\zeta_m}, Q_{\zeta_n}\} = \delta_{\zeta_m} Q_{\zeta_n} \tag{2.15}$$

This is the asymptotic charge algebra and is represented by the Dirac algebra up to a central term [35].

$$\{Q_{\zeta_m}, Q_{\zeta_n}\}_{DB} = Q_{[\zeta_m,\zeta_n]} + \frac{1}{8\pi G}\int_{\partial\Sigma} k_\zeta[\mathcal{L}_{\zeta_n}\bar{g}, \bar{g}]. \tag{2.16}$$

The $2nd$ term in (2.16) is the central term we referred to above. In order to proceed further and compute the central term we need the Lie derivatives of the NHEK region and they are [6],

$$\mathcal{L}_{\zeta_n}\bar{g}_{\tau\tau} = 4GJ\Omega^2(1-\Lambda^2)r^2 in^{-in\varphi}, \tag{2.17}$$

$$\mathcal{L}_{\zeta_n}\bar{g}_{r\varphi} = -\frac{2GJ\Omega^2 r}{1+r^2}n^2 e^{-in\varphi}, \tag{2.18}$$

$$\mathcal{L}_{\zeta_n}\bar{g}_{\varphi\varphi} = 4GJ\Lambda^2\Omega^2 ine^{-in\varphi}, \tag{2.19}$$

$$\mathcal{L}_{\zeta_n}\bar{g}_{rr} = -\frac{4GJ\Omega^2}{(1+r^2)^2}ine^{-in\varphi} \tag{2.20}$$

From the Lie derivatives, the central term has been shown to be [6],

$$\frac{1}{8\pi G}\int_{\partial\Sigma} k_\zeta[\mathcal{L}_{\zeta_n}\bar{g}, \bar{g}] = -i(m^3+2m)\delta_{m+n}J \tag{2.21}$$

The relating of the central term to the angular momentum is not unique to NHEK as it is a consequence of the ASG analysis of the AdS_3 spacetime. To arrive at a point where the the Dirac bracket can be related to commutators, a dimensionless entity needs to introduced which relates the the charge to the operator L_n. This entity takes the form of [6, 37],

$$\hbar L_n \equiv Q_{\zeta_n} + \frac{3J}{2}\delta_n. \tag{2.22}$$

Using the rule that relates the commutators to the Dirac bracket,

$$\{x, y\}_{D.B} = \frac{i}{\hbar}[x, y] \tag{2.23}$$

The central charge can then be read off the quantum charge algebra,

$$[L_m, L_n] = (m-n)L_{m+n} + \frac{J}{\hbar}m(m^2-1)\delta_{m+n,0} \tag{2.24}$$

The expression (2.24) is the Virasoro algebra associated with 2D CFT. The appearance of the Virasoro algebra following the computation of the asymptotic symmetry algebra associated with the NHEK region is a statement that the NHEK region is dual to a 2D CFT. A discussion of the Virasoro algebra is provided in 2.1.5. The central charge for the NHEK geometry is then,

$$c_L = \frac{12J}{\hbar}. \tag{2.25}$$

2.1.4 Microscopic Thermodynamics

The central charge ultimately enables us to work-out the thermodynamics of the NHEK geometry. This process begins with finding an expression for the microscopic temperature. One of the challenges with determining microscopic temperature is the need to have a quantum vacuum in the region being investigated. The challenge posed by the Kerr black hole in so far as the defining a quantum vacuum is that it does not have a quantum state defined everywhere. This is a consequence of the fact that the Kerr black hole does not have a timelike vector defined everywhere. The Kerr timelike vector is only defined in the region $r > 0$, in this region we don't encounter closed timelike curves. However if one approaches the region $r < 0$, then one encounters closed timelike curves.

To counter this challenge of the Kerr solution not having a quantum state defined everywhere, the approach of Frolov-Thorne is taken. The objective of this approach is to ultimately arrive at a place where we have a quantum vacuum state for the NHEK geometry. The process of defining this (Frolov-Thorne) vacuum involves defining scalar quantum field with eigenstates of asymptotic energy and angular momentum. This scalar field is defined in the near horizon outside the black hole. Outside the horizon of the Kerr black we have a mixed state and not a pure quantum, which then necessitates that we undergo this process of defining a Frolov-Thorne vacuum.

One then proceeds to look into the interior of the black hole to arrive at a vacuum state. This vacuum can then be expressed as a density matrix in the eigenbasis of the scalar field. The expression for the eigenbasis is of the form,

$$e^{\hbar \frac{\omega - \Omega_H m}{T_H}} \tag{2.26}$$

The eigenbasis are a function of the Boltzmann constant and the Hawking temperature (T_H). The m is the angular momentum and ω is the asymptotic energy. Given that the Hawking temperature for extremal the Kerr approaches zero, the expression for the density becomes unusable.

To counter this challenge, one introduces a change of coordinates which result in the removal of dependence of the eigenbasis from the Boltzmann constant to the right and left moving charges and also the left and right moving temperatures. With the right and left moving temperatures defined as,

$$T_L = \frac{r_+ - M}{2\pi(r_+ - (J/M))}, \quad T_R = \frac{r_+ - M}{2\pi\lambda r_+}. \tag{2.27}$$

From this point, one then imposes the extremality condition and we arrive at the value of the left moving temperature to be,

$$T_L = \frac{1}{2\pi}. \tag{2.28}$$

With the right moving temperature becoming zero ($T_R = 0$).

The next step in the process is to work out the microscopic entropy. This is done using the Cardy formula by employing the the expressions for left moving temperature (T_L) and the central charge (c_L). However before providing the entropy computation and the results, we digress briefly and look at 2D Chiral CFT.

2.1.5 Chiral 2D CFT

The authors of [6] argued that the extreme Kerr geometry is dual to a chiral 2D CFT. Below we present a summary of the key properties of 2D CFTs, and we will also provide an argument contained in [6] of why the extreme Kerr geometry is dual specifically to a chiral 2D CFT.

As a starting point we will mention that there is no standard 2D CFT, the authors of [6] admitted that the central charge derived in their paper tells us very little about the nature of the 2D CFT.

A 2D CFT is defined as a local quantum field theory with local conformal invariance [35, 29]. In two dimensions, the local conformal group is an infinite-dimensional extension of the globally-defined conformal group $SL(2,\mathbb{R})_L \times SL(2,\mathbb{R})_R$ on the plane or the cylinder [35]. It is generated by two sets of vector fields, $L_n, \bar{L}_n, n \in \mathbb{Z}$. These vector fields obey the Witt algebra [35, 29],

$$\begin{aligned}
[L_m, L_n] &= (m-n)L_{m+n}, \\
[L_m, \bar{L}_n] &= 0 \\
[\bar{L}_m, \bar{L}_n] &= (m-n)\bar{L}_{m+n}
\end{aligned} \tag{2.29}$$

Using Noether's theorem, each symmetry can be associated with a quantum operator. The local conformal symmetry is related to the conserved and trace-less stress-energy tensor operator. The stress-energy tensor can be decomposed into the right and left moving modes $\mathcal{L}_n$ and $\bar{\mathcal{L}}_n$. The operators $\mathcal{L}_n, \bar{\mathcal{L}}_n$ form two copies of the Virasoro algebra [35]

$$[\mathcal{L}_m, \mathcal{L}_n] = (m-n)\mathcal{L}_{m+n} + \frac{c_L}{12}m(m^2 - A_L)\delta_{m+n,0}, \tag{2.30}$$

$$[\mathcal{L}_m, \bar{\mathcal{L}}_n] = 0$$

$$[\bar{\mathcal{L}}_m, \bar{\mathcal{L}}_n] = (m-n)\bar{\mathcal{L}}_{m+n} + \frac{c_R}{12}m(m^2 - A_R)\delta_{m+n,0}. \tag{2.31}$$

The $\mathcal{L}_{-1}, \mathcal{L}_0, \mathcal{L}_1$ and $\bar{\mathcal{L}}_{-1}, \bar{\mathcal{L}}_0, \bar{\mathcal{L}}_1$ span the $SL(2,\mathbb{R})$ subalgebra. The numbers c_L and c_R give us the left and the right moving central charges of the CFT. In section 2.1.3 we saw the value of c_L being read-off as (2.25). The auxiliary parameters A_L and A_R depend on whether the CFT is defined on a cylinder or on the plane. These parameters gives us insight into the shifts in the background of the zero eigen-modes $\mathcal{L}_0, \bar{\mathcal{L}}_0$. The central charges need to be taken to be large for any gravitational dual to be admissible [35]. For a detailed discussion of the 2D CFT and the Virasoro algebra the reader is encouranged to see [29, 17, 16].

As we mentioned earlier in the work [6, 34] the authors state that it is expected that the extreme Kerr geometry should be dual to a chiral 2D CFT. The argument for this goes as follows; at extremality the rotational velocity of the Kerr black hole horizon becomes the speed of light. This results in both edges of the forward light cone coinciding as the horizon is approached and forces all physical excitations, which must be between the edges of the light cone, to spin around chirally with the black hole [6].

2.1.5.1 Cardy formula

The expression for the central charge and the left moving temperature are used to determine the entropy of extreme Kerr geometry by employing the Cardy formula. The Cardy formula relates the entropy of a 2D conformal theory with its central charge. The formula was initially limited to 2D conformal theory, however in 2000 it was shown to be valid in $(n+1)$ dimensional conformal theory [38] The original formula took the form of,

$$S = 2\pi\sqrt{\frac{c}{6}\Big(L_0 - \frac{c}{24}\Big)}. \tag{2.32}$$

Where L_0 is the product of the total energy and the radius. The shift of $\frac{c}{24}$ is caused by the Casimir effect. Using the relationship between the total energy and the temperature, the formula can be recast into a form we are familiar with i.e. [35],

$$S_{CFT} = \frac{\pi^2}{3}(c_L T_L + c_R T_R) \tag{2.33}$$

Both [6] and [39] have assumed the applicability of the Cardy formula to the extreme Kerr geometry. There is an instructive discussion in [35] on why the Cardy formula should not necessarily be applicable to the extreme Kerr geometry, and the sort of assumptions one needs to make for it to be applicable to extreme Kerr. Typically the Cardy formula holds in the ranges

$$T_L > \frac{1}{2\pi}, \quad T_R > \frac{1}{2\pi}. \tag{2.34}$$

As we saw in the above discussion on the derivation of the left moving temperature both the left and right moving temperature associated with vacuum extreme Kerr geometry state do not fall within this range. There are two cases where it has been shown that the Cardy formula remains relevant even when this range has been extended [35].

- Extended validity for large central charge and sparse light spectrum
- Extended validity for long strings

The first of these extensions is the one that makes the application of the Cardy formula to the extreme Kerr geometry valid. The validity of this argument follows from the study of symmetric orbifold theories. These theories can be thought of as a sigma model with target space being some four-manifold, $\mathcal{M}_4$ identified up to permutations. In this regard, the symmetric orbifold theory is a CFT and has central charge c_{sym}. Now if instead of having one target space $\mathcal{M}$, we have a sigma model with N identical copies of the manifold, $\mathcal{M}$ as the target space, we end up with a symmetric product orbifold theory. In [40] it was shown that symmetric orbifold theories are consistent with the bounds which render the Cardy formula meaningful, this was shown in the range of large c.

The extreme Kerr geometry has also been shown to contain a warped deformation of the self dual orbifold. A self dual orbifold is best described by looking at a $3d$ black hole in the form of a BTZ black hole. This black hole is described by its mass M and angular momentun J. It has two extremal limits defined as $Ml = \pm J$. In both the extremal limits, the near horizon geometry has an $SL(2,\mathbb{R}) \times U(1)$ isometry group given by,

$$ds^2 = \frac{l^2}{4}\Big(- r^2 dt^2 + \frac{dr^2}{r^2} + 2|J|(d\phi + \frac{r}{2|J|}dt)^2\Big) \tag{2.35}$$

where $\phi \approx \phi + 2\pi$. This then is known as the self-dual AdS_3 orbifold. Hence one can think of it as an isometry group associated with the near horizon extreme geometry of the BTZ black hole in $3d$. This self dual orbifold is often referred to as the "very-near-horizon" of the near horizon limit. This near horizon limit consists of AdS_2 with a twisted $U(1)$ fibre.[35, 41].

The derivation of the Kerr/CFT correspondence followed from the result that the self dual orbifold ("the very near-horizon limit") contains one copy of the Virasoro algebra as an asymptotic algebra which extends the $U(1)$ rotational symmetry. The entropy of the very near horizon is reproduced by a chiral half of the Cardy's formula, stemming from the 2D CFT [35].

2.1.5.2 Cardy Entropy: A comparison with the Bekenstein-Hawking-Kerr

In this section the expression for the entropy using the Cardy formula is compared with the values of the entropy for extreme Kerr geometry determined using the Bekenstein-Hawking approach.

The microscopic entropy of the NHEK region using the Cardy formula is,

$$S = \frac{\pi^2}{3} c_L T_L = \frac{2\pi J}{\hbar} \tag{2.36}$$

Next we want to compare this result to that obtained using the Bekenstein-Hawking approach. The expression for the Bekenstein-Hawking entropy is,

$$S_{BH} = \frac{Area}{4\hbar G} \tag{2.37}$$

We start with the computation of the area of the event horizon of the Kerr black hole. The expression for the area computed at the the outer event horizon ($r = r_+$) is [25];

$$\begin{aligned} A_H &= \int_{r=r_+} \sqrt{g_{\theta\theta} g_{\phi\phi}} d\theta d\phi \\ &= (r_+^2 + (J/M)^2) \int_0^{2\pi} d\theta \int_0^{\pi} \sin\theta d\theta \\ &= 4\pi (r_+^2 + (J/M)^2) \end{aligned} \tag{2.38}$$

And using the expression for maximal angular momentum associated with the extreme Kerr geometry,

$$J = GM^2, \tag{2.39}$$

and the fact that at extremality, $r_+ = GM$, the area of the event horizon can be expressed as,

$$\mathcal{A}_H = 16\pi(GM)^2. \tag{2.40}$$

Now we take this and plug into the the Bekenstein-Hawking entropy, and arrive at the following expression for entropy,

$$\begin{aligned} S_{BH} &= \frac{Area}{4\hbar G} \\ &= \frac{2\pi(GM)^2}{\hbar G} \\ &= \frac{2\pi GM^2}{\hbar} \\ &= \frac{2\pi J}{\hbar}. \end{aligned} \tag{2.41}$$

The expression (2.41) is identical to (2.36) [6]. In the next section our focus shifts to the derivation of the hidden conformal symmetries associated with the Kerr black hole solution. Again we follow the work by Strominger et al, albeit in a different paper [42].

2.2 Hidden Symmetries of the Near Region of the Kerr black hole

The near region of the Kerr black hole has been shown to have conformal symmetries of the a 2D CFT. These symmetries are not immediately evident when one looks at the metric of the Kerr black hole (2.1). These symmetries are evident when an obeserver approaches the horizon of the black hole, but not necessarily arriving at the near horizon we discussed in the previous section. To arrive at a point where can see these symmetries we need to define conformal coordinates which we can map to the Laplacian of the scalar field in the near regions of the Kerr black hole. Once we have mapped these conformal coordinate to the Laplacian, we will then be able to see that the Laplacian can be expressed as the Casimir of the $SL(2,\mathbb{R})_L \times SL(2,\mathbb{R})_R$. We start by reviewing the conformal coordinates of [6].

2.2.1 Conformal Coordinates

The conformal coordinate employed in the analysis of the near region obey the algebra of the $SL(2,\mathbb{R})$ group. We will see that these coordinate will generate two copies of the $SL(2,\mathbb{R})$ algebra, i.e. will be consistent with the $SL(2,\mathbb{R})_L \times SL(2,\mathbb{R})_R$. The conformal coordinates are defined as [42],

$$\omega^+ = \sqrt{\frac{r-r_+}{r-r_-}}e^{2\pi T_R\phi}$$
$$\omega^- = \sqrt{\frac{r-r_+}{r-r_-}}e^{2\pi T_L\phi-\frac{t}{2M}}$$
$$y = \sqrt{\frac{r_+-r_-}{r-r_-}}e^{\pi(T_L+T_R)\phi-\frac{t}{4M}} \tag{2.42}$$

The right and left moving temperatures are further defined as,

$$T_R \equiv \frac{r_+-r_-}{4\pi a}, \qquad T_L \equiv \frac{r_++r_-}{4\pi a} \tag{2.43}$$

In the above, a is related to the angular momentum of the Kerr black hole as, $a = J/M$. As we can see, these coordinates are mapped to the variables t, ϕ and r variables which we find in the Kerr metric. Next we need to see if we can find vector fields associated with these coordinates which can be seen as generators of a conformal group, in our case a 2D CFT. These vector fields are locally defined and are,

$$H_1 = i\partial_+, \tag{2.44}$$
$$H_0 = i(\omega^+\partial_+ + \frac{1}{2}y\partial_y),$$
$$H_{-1} = i(\omega^{+2}\partial_+ + \omega^+ y\partial_y - y^2\partial_-)$$

and,

$$\bar{H}_1 = i\partial_-, \tag{2.45}$$
$$\bar{H}_0 = i(\omega^-\partial_- + \frac{1}{2}y\partial_y),$$
$$\bar{H}_{-1} = i(\omega^{-2}\partial_- + \omega^- y\partial_y - y^2\partial_+).$$

Both the $H_0, H_{\pm1}$ and the $\bar{H}_0, \bar{H}_{\pm1}$ obey the $SL(2,\mathbb{R})$ algebra.

$$[H_0, H_{\pm1}] = \mp iH_{\pm1}, \qquad [H_{-1}, H_1] = -2iH_0. \tag{2.46}$$

From these vector fields we can construct the quadratic Casimir of the $SL(2,\mathbb{R})$ group. And the Casimir in the conformal coordinates takes the form of,

$$\mathcal{H}^2 = \bar{\mathcal{H}}^2 = -H_0^2 + \frac{1}{2}(H_1H_{-1} + H_{-1}H_1)$$
$$= \frac{1}{4}(y^2\partial_y^2 - y\partial_y) + y^2\partial_+\partial_-. \tag{2.47}$$

A discussion on what is a quadratic Casimir for the $SL(2,\mathbb{R})$ is provided in appendix B. For now, suffice it is to say that the Casimir is the centre element of the group and commutes with all the generators of the group. In the case of the $SL(2,\mathbb{R})$ it can also be expressed as the Laplacian as we will see in the next section.

2.2.2 Mapping the scalar wave equation to a 2D CFT

We begin this section by studying the massless Klein-Gordon equation of the Kerr black hole solution. We will then vary the Laplacian to work out the the massless scalar wave equation in the near region of the Kerr black hole.

The expression for the massless Klein-Gordon equation is,

$$\frac{1}{\sqrt{-g}}\partial_\mu(\sqrt{-g}g^{\mu\nu}\partial_\nu\Phi) = 0. \tag{2.48}$$

We then try the following ansatz as a possible solution to the (2.48),

$$\Phi(t, r, \theta, \phi) = e^{-i\omega t + im\phi}\Phi(r, \theta). \tag{2.49}$$

This is an expression of the eigenmodes associated with the Klein-Gordon equation. What makes the Kerr metric interesting and useful to study is the result that the Laplacian of the Kerr metric is fully separable. Expanding (2.48) we get the Laplacian in the form of,

$$\begin{aligned}&\partial_r(\Delta\partial_r\Phi) + \frac{(2Mr_+\omega - (J/M)m)^2}{(r-r_+)(r_+-r_-)}\Phi - \frac{(2Mr_-\omega - (J/M)m)^2}{(r-r_-)(r_+-r_-)}\Phi \\ &+ (r^2 + (J/M)^2\cos^2\theta + 2M(r+2M))\omega^2\Phi + \nabla_{S^2}\Phi = 0.\end{aligned} \tag{2.50}$$

Where Δ is the same as in (2.2), $\Delta = r^2 + (J/M)^2 - 2Mr$. As stated above the above equation (2.50) is fully separable. To proceed, we further separate the (2.49) into the radial and angular parts. The ansatz then takes the form of,

$$\Phi(t, r, \theta, \phi) = e^{-i\omega t + im\phi}R(r)S(\theta). \tag{2.51}$$

.

Equation (2.51) expresses the seperation of the radial and the angular part of the Laplacian. The radial part of the Laplacian then becomes,

$$\begin{aligned}&\Big[\partial_r\Delta\partial_r + \frac{(2Mr_+\omega - (J/M)m)^2}{(r-r_+)(r_+-r_-)} - \frac{(2Mr_-\omega - (J/M)m)^2}{(r-r_-)(r_+-r_-)} \\ &+ (r^2 + 2M(r+2M))\omega^2\Big]R(r) = K_\ell R(r).\end{aligned} \tag{2.52}$$

The angular equation on the other hand, has the expression,

$$\Big[\frac{1}{\sin\theta}\partial_\theta(\sin\theta\partial_\theta) - \frac{m^2}{\sin^2\theta} + \omega^2(J/M)^2\cos^2\theta\Big]S(\theta) = -K_\ell S(\theta) \tag{2.53}$$

Where K_ℓ is the separation constant. We are interested in studying the symmetries of the Kerr black hole beyond the radius of the event horizon. When we ignore the terms with ω^2, this enables us to focus on the region where excitation of the scalar wave equation are greater than the radius of the black hole. This happens in the region where $\omega r \ll 1$. This region can be further divided into the "near" and the "far" region. Theses regions are formally defined as [42],

$$\begin{aligned} r &\ll \frac{1}{\omega} \quad Near, \\ r &\gg M \quad Far. \end{aligned} \tag{2.54}$$

Our interest is in the near region. This near region is not the same as the HENKE region associated with the strong Kerr/CFT correspondence. A distant observer in the near region would still be at some distance away from NHEK region of the black hole. The radial equation then becomes,

$$\Big[\partial_r \Delta \partial_r + \frac{(2Mr_+\omega - (J/M)m)^2}{(r-r_+)(r_+-r_-)} - \frac{(2Mr_-\omega - (J/M)m)^2}{(r-r_-)(r_+-r_-)}\Big] R(r) = \ell(\ell+1)R(r) \tag{2.55}$$

The solutions to (2.55) are hypergeometric functions, which as we know can be viewed as representation of the $SL(2,\mathbb{R})$. The analysis does not end here however, we proceed by restating the vector fields (2.44) and (2.45) in the familiar (r, ϕ, t) coordinates.

$$\begin{aligned} H_1 &= ie^{-2\pi T_R \phi}\Big(\Delta^{1/2}\partial_r + \frac{1}{2\pi T_R}\frac{r-M}{\Delta^{1/2}}\partial_\phi + \frac{2T_L}{T_R}\frac{Mr-(J/M)^2}{\Delta^{1/2}}\Big), \\ H_0 &= \frac{i}{2\pi T_R}\partial_\phi + 2iM\frac{T_L}{T_R}\partial_t, \\ H_{-1} &= ie^{2\pi T_R \phi}\Big(-\Delta^{1/2}\partial_r + \frac{1}{2\pi T_R}\frac{r-M}{\Delta^{1/2}}\partial\phi - \frac{2T_L}{T_R}\frac{Mr-(J/M)^2}{\Delta^{1/2}}\partial_t\Big) \end{aligned} \tag{2.56}$$

and,

$$\begin{aligned} \bar{H}_1 &= ie^{-2\pi T_L \phi + t/2M}\Big(\Delta^{1/2}\partial_r - \frac{J/M}{\Delta^{1/2}}\partial_\phi - 2M\frac{r}{\Delta^{1/2}}\partial_t\Big), \\ \bar{H}_0 &= -2iM\partial_t, \\ \bar{H}_{-1} &= ie^{2\pi T_L \phi - t/2M}\Big(-\Delta^{1/2}\partial_r - \frac{J/M}{\Delta^{1/2}}\partial_\phi - 2M\frac{r}{\Delta^{1/2}}\partial_t\Big). \end{aligned} \tag{2.57}$$

And the quadratic Casimir is these coordinates is,

$$\mathcal{H}^2 = \partial_r \Delta \partial_r - \frac{(2Mr_+\partial_t + (J/M)\partial_\phi)^2}{(r-r_+)(r_+-r_-)} + \frac{(2Mr_-\partial t + (J/M)\partial_\phi)^2}{(r-r_-)(r_+-r_-)} \tag{2.58}$$

From this point it becomes a fairly easy exercise to see the radial part of the Laplacian (2.55) as the quadratic Casimir (2.58); these two expression are very similar. From this observation we can conclude that the radial part of the Laplacian of the Kerr black hole in the near region is the centre element of the $SL(2,\mathbb{R})$. This allows us to conclude that the near region of the Kerr black has symmetries of the $SL(2,\mathbb{R})$ group. Given that we have the left and the right moving sectors, this means that the near region has symmetries of the $SL(2,\mathbb{R})_L \times SL(2,\mathbb{R})_R$ group. This is the group of associated with a 2D CFTs.

The $SL(2,\mathbb{R})_L \times SL(2,\mathbb{R})_R$ symmetry is not a global symmetry, it is limited to the near region of the black hole. When one moves away from the near region the symmetry is broken by the periodicity of the ϕ coordinate of the $SL(2,\mathbb{R})_L \times SL(2,\mathbb{R})_R$ group. This periodicity can be expressed as,

$$\phi \sim \phi + 2\pi. \tag{2.59}$$

The breaking of the symmetry in this manner is often referred to as a spontaneous symmetry breaking. Under the periodic identification (2.59), the conformal coordinates are transformed into the form,

$$\omega^+ \sim e^{4\pi^2 T_R}\omega^+, \quad \omega^- \sim e^{4\pi^2 T_L}\omega^-, \quad y \sim e^{2\pi^2(T_L+T_R)}y. \tag{2.60}$$

This identification of the conformal coordinates is a group element and is generated,

$$g = e^{-i4\pi^2 T_R H_0 - i4\pi^2 T_L \bar{H}_0}, \quad g \in SL(2,\mathbb{R})_L \times SL(2,\mathbb{R})_R. \tag{2.61}$$

This results in the $SL(2,\mathbb{R})_L \times SL(2,\mathbb{R})_R$ group becoming the $U(1)_L \times U(1)_R$ group [37].

2.2.3 Conformal Weights

To begin the discussion on conformal weights we need to state what weights are. Given a representation of the group, the weights can be thought of as the eigenvalues associated with the action of a group on some field. In the context of the $SL(2,\mathbb{R})$, when H_0 acts on some field, the associated eigenvalue h_L is an left moving weight. And similarly when $\bar{H}_0$ is the right moving weight, i.e.,

$$H_0\Phi = h_L\Phi \tag{2.62}$$

$$\bar{H}_0\Phi = h_R\Phi \tag{2.63}$$

We can work out the highest weight by acting on our field by H_1 and $\bar{H}_1$. When acting on the field by the highest weight state, we should have a relation,

$$H_1\Phi = 0 \quad \bar{H}_0\Phi = 0 \tag{2.64}$$

Using the definition of H_1 and $\bar{H}_1$ given in (2.42) we can see that our Φ can only depend on y. From this we can see that the action of H_0 and $\bar{H}_0$ are essentially the same action, i.e.,

$$iH_0\Phi(y) = h_L\Phi(y) = i\bar{H}_0\Phi(y) = h_R\Phi(y) \tag{2.65}$$

We introduced the complex number (i) to ensure consistency with the formal $SL(2,\mathbb{R})$ algebra. If we let $h_L = h_R = h$, then we have,

$$H_0\Phi(y) = \frac{1}{2}y\partial_y\Phi(y) = -h\Phi(y) \tag{2.66}$$

The solution to the differential equation (2.66) is of the form,

$$\Phi(y) = C_1 y^{-2h}, \tag{2.67}$$

where C_1 is an arbitrary constant. From here we conduct a similar analysis for the quadratic Casimir. From 2.47 we have the below expression for the Casimir,

$$\begin{aligned}\mathcal{H}^2\Phi(y) &= \ell(\ell+1)\Phi(y)\\ &= \frac{1}{4}\Big(y^2\partial_y^2 - y\partial_y\Big)\Phi(y)\end{aligned} \tag{2.68}$$

The solution to above equation takes is of the form,

$$\Phi(y) = C_2 y^{1-\sqrt{1+4(\ell(\ell+1))^2}}. \tag{2.69}$$

Again we have C_2 as a constant. From here we can compare the equations (2.67) and (2.69). From the comparison we see the weights are related to ℓ by the equation,

$$h = \frac{1}{2}\sqrt{1+4(\ell(\ell+1))^2} - 1). \tag{2.70}$$

This expression suggests that we are dealing the maximum eigenvalue of H_0 and $\bar{H}_0$ which is is the highest weight state. Simplifying the above expression (2.70) we have,

$$(h(h+1))^2 = (\ell(\ell+1))^2. \tag{2.71}$$

This allows us to see and to conclude that,

$$h_L = h_R = h = \ell. \tag{2.72}$$

2.2.4 Microscopic Thermodynamics of the Hidden Conformal Symmetry

To work out the microscopic entropy we will need to assume that the there is a 2D CFT in the near region of the Kerr black hole. This seems like a plausible assumption given that the the $SL(2,\mathbb{R})$ is associated with 2D CFTs. Furthermore, we need assume that the there is continuity in the charge distribution between the near region of the Kerr black hole and the NHEK region. Based on this assumption we can proceed to employ the Cardy formula in determining the microscopic temperature.

The central charge for the extreme Kerr black hole was shown to be,

$$c_R = c_L = 12J \tag{2.73}$$

From here we can take the left and the right moving temperature (2.43) and compute the entropy. The expression for the entropy is then,

$$\begin{aligned}S &= \frac{\pi^2}{3}12J\Big(\frac{r_+ + r_-}{4\pi(J/M)} + \frac{r_+ - r_-}{4\pi(J/M)}\Big)\\ &= \frac{2\pi r_+ J}{(J/M)}\\ &= 2\pi M r_+\end{aligned} \tag{2.74}$$

When we compare this expression of the microscopic entropy to that computed using the Bekenstein-Hawking formula,

$$S_{BH} = 2\pi M r_+ \tag{2.75}$$

There is agreement between the two. This was of a somewhat surprising result as the temperature used in the entropy computation using the Cardy formula largely relied on the symmetries of the near region and not on the analysis of the asymptotic symmetries which where shown to be dual 2D CFT [37].

This concludes our review of Kerr/CFT within the NHEK geometry as well the hidden conformal symmetries associated with the near region of the Kerr black hole. In the next section we review and briefly discuss black rings, their properties as well as the challenges associated with their unique topology.

3

Black Rings

Although we have known about the 5d Kerr black hole solution to Einstein equations since 1986, black rings were only discovered as recently as 2001 [43]. These black objects exist in $D \geq 5$ dimensions and in five dimensions have an event horizon which has an $S^1 \times S^2$ topology, where S^1 is a circle and S^2 a 2-sphere.

In this chapter we provide a high-level review of black rings. We start with the black ring coordinate system, then proceed to discuss the neutral black ring and then we briefly discuss a few of their properties. The properties we discuss are specifically applicable to the neutral singly rotating black ring. Lastly we will look at the super-symmetric black ring solution in 5-d and its near horizon geometry.

3.1 Black Ring Coordinate System

The ring can be compared to a circular string that acts as an electric source of the 3-form field strength $H = dB$. The field strength satisfies the field equations [43]:

$$\partial_\mu(\sqrt{-g}H^{\mu\nu\rho}) = 0 \tag{3.1}$$

The coordinates which describe the ring in flat spacetime are, [43],

$$ds^2 = dr_1^2 + r_1^2 d\phi^2 + dr_2^2 + r_2^2 d\psi^2. \tag{3.2}$$

Using the analogy of a a circular string with a single electric source stated above, the magnetic field at $r_1 = 0$ and $r_2 = R$ and $0 \leq \psi \leq 2\pi$, would then be given by,

$$B_{t\psi} = \frac{R}{2\pi}\int_0^{2\pi} d\psi \frac{r_2 \cos\psi}{r_1^2 + r_2^2 + R^2 - 2Rr_2\cos\psi} \tag{3.3}$$

$$= -\frac{1}{2}\left(1 - \frac{R^2 + r_1^2 + r_2^2}{\Sigma}\right), \tag{3.4}$$

where

$$\Sigma = \sqrt{(r_1^2 + r_2^2 + R^2)^2 - 4R^2 r_2^2}. \tag{3.5}$$

The circular string would then have an electric-magnetic dual to this field in 5d, $*H = F = dA$, which is a one-form potential. The surface of constant A_ϕ is orthogonal to surfaces of constant $B_{t\psi}$. The dual field then becomes:

$$A_\phi = -\frac{1}{2}\left(1 + \frac{R^2 - r_1^2 - r_2^2}{\Sigma}\right) \tag{3.6}$$

For constant values of $B_{t\psi}$ and A_ϕ, the following coordinates are defined;

$$y = -\frac{R^2 + r_1^2 + r_2^2}{\Sigma}, \tag{3.7}$$

$$x = \frac{R^2 - r_1^2 - r_2^2}{\Sigma}. \tag{3.8}$$

With the inverse,

$$r_1 = R\frac{\sqrt{1 - x^2}}{x - y}, \tag{3.9}$$

$$r_2 = R\frac{\sqrt{y^2 - 1}}{x - y}. \tag{3.10}$$

The ranges of y and x are;

$$-\infty \leq y \leq -1, \qquad -1 \leq x \leq 1. \tag{3.11}$$

While $y = -\infty$ corresponds to the location of the ring source, asymptotic infinity is recovered as $x \to y \to -1$. The axis of rotation around ψ (which can be viewed as a plane) occurs with $r_2 = 0$ at $y = -1$. The axis of rotation in the ϕ direction occurs at $r_1 = 0$. This can be separated into two areas; $x = 1$ is the disk with $r_2 \leq R$, and $x = -1$ is outside the ring, with $r_2 \geq R$. The flat metric is then:

$$ds^2 = \frac{R^2}{(x - y)^2}\left[(y^2 - 1)d\psi^2 + \frac{dy^2}{y^2 - 1} + \frac{dx^2}{1 - x^2} + (1 - x^2)d\phi^2\right] \tag{3.12}$$

The above metric can be reconfigured to better describe the spacetime in the region near the ring by introducing the following coordinate transformation:

$$r = -\frac{R}{y}, \qquad \cos\theta = x. \tag{3.13}$$

The coordinates have the following ranges,

$$0 \leq r \leq R \tag{3.14}$$

$$0 \leq \theta \leq \pi. \tag{3.15}$$

The flat metric is then given by,

$$ds^2 = \frac{1}{(1 + \frac{\cos\theta}{R})^2}\left[\left(1 - \frac{r^2}{R^2}\right)R^2 d\psi^2 + \frac{dr^2}{1 - r^2/R^2} + r^2(d\theta^2 + \sin^2\theta d\phi^2)\right]. \tag{3.16}$$

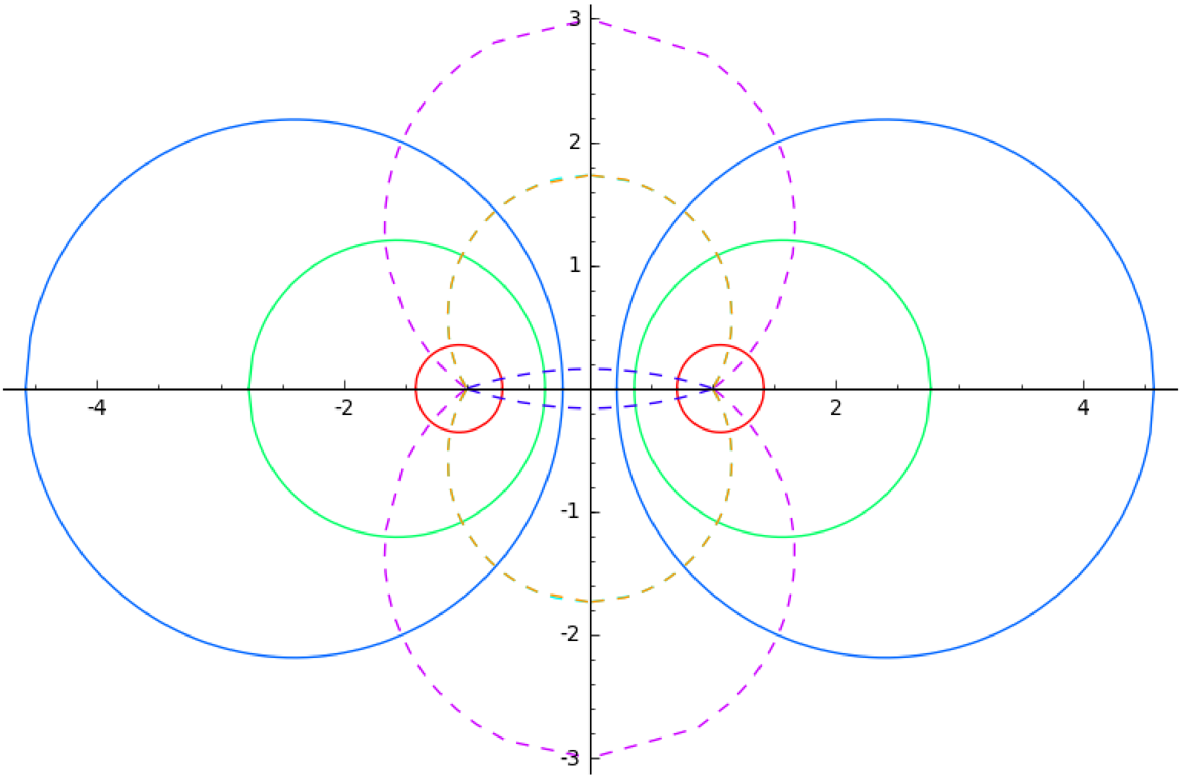

Figure 3.1: Black ring coordinates for flat 4-d space. These are at constant $\phi(\phi+\pi)$ and $\psi(\psi+\pi)$. The dashed lines are spheres at constant $|x|\ \epsilon\ [0,1]$. The solid circles to spheres at constant $y\ \epsilon\ [-\infty,-1]$

In concluding this brief discussion on the black ring coordinate system, we note the following; there is a singularity at $r=R$ corresponding to the ψ-axis of rotation. We also observe that at constant r, i.e., constant y, the surface will have a topology $S^2\times S^1$. The S^2 is parametrised by (ϕ,θ) and S^1 by ψ. The horizon of the ring will be at constant values of y or r. Lastly, the (x,y) coordinates used in the two-form potential B, are also useful in the analysis of the super-symmetric black ring [43] which is discussed in section 3.5 below.

3.2 Neutral Black Ring

The neutral single rotating black ring solution is arguably the simplest formulation of the known black ring solutions. The metric takes the form [43, 44];

$$ds^2=-\frac{F(y)}{F(x)}\Big(dt-CR\frac{1+y}{F(y)}d\psi\Big)^2+\frac{R^2}{(x-y)^2}F(x)\Big[-\frac{G(y)}{F(y)}d\psi^2-\frac{dy^2}{G(y)}+\frac{dx^2}{G(x)}+\frac{G(x)}{F(x)}d\phi^2\Big] \quad (3.17)$$

with,

$$F(\xi)=1+\lambda\xi, \qquad G(\xi)=(1-\xi^2)(1+\nu\xi), \quad (3.18)$$

and,

$$C=\sqrt{\lambda(\lambda-\nu)\frac{1+\lambda}{1-\lambda}}. \quad (3.19)$$

The parameters λ and ν are dimensionless and have the range,

$$0<\nu\leq\lambda<1. \quad (3.20)$$

The parameters λ and ν provide insight into the shape and the rotation velocity of the black ring. It easy to see that when they are both set to zero, we recover the flat metric (3.16).

The metric has a singularity at $y = 1/\nu$, however this is a coordinate singularity which can be removed by transforming $(t, \psi) \to (v, \psi')$ as [43],

$$dt = dv - CR\frac{1+y}{G(y)\sqrt{-F(y)}}dy \qquad d\psi = d\psi' + \frac{\sqrt{-F(y)}}{G(y)}dy. \tag{3.21}$$

This transforms the metric 3.17 into,

$$ds^2 = -\frac{F(y)}{F(x)}\Big(dv - CR\frac{1+y}{F(y)}d\psi'\Big)^2 + \frac{R^2}{(x-y)^2}F(x)\Big[-\frac{G(y)}{F(y)}d\psi'^2 - \frac{d\psi' dy}{\sqrt{-F(y)}} + \frac{dx^2}{G(x)} + \frac{G(x)}{F(x)}d\phi^2\Big].$$

The horizon has the topology of $S^1 \times S^2$. The S^1 is parametrised by ψ and S^2 by (ϕ, θ). The S^2 is not a perfect sphere, it is somewhat distorted. At $y = -\infty$ we have an inner spacelike singularity [43].

3.3 Black Ring Properties

One of the key properties of the black ring solutions is that they offer us proof that the no hair principle is violated in dimensions $D \geq 5$. This is seen through studying their two conserved charges namely; spin and mass. These are determined by analysing what happens to the metric near asymptotic infinity $x \to y \to -1$.

What was shown in [43] was that for certain values of j, the reduced spin, one finds a Myers-Perry black hole and two black rings all with the same values of spin and mass. This they observed in the range $27/32 \leq j^2 < 1$. Furthermore, they found that the angular momentum (for fixed mass) of the black ring was bounded from below and not from above. This is specifically applicable to the neutral singly rotating black ring [43].

However, in [44] it was shown that there is a special class of charged singly rotating black ring solutions whose angular momentum was bounded from above and whose extremal limit could be determined. Furthermore, in [45] the authors showed that the black ring with two angular momenta is bounded from above and has an extremal limit. For further reading and detailed analysis of black ring properties please see [43, 44, 45, 46].

3.4 Separability and non-extremal black rings

A statement that is often made in the literature on black rings is that applying the separation of variables techniques to the scalar wave equation of the neutral black ring solution is extremely difficult, even impossible. Two examples of this statement can be found in [43], and [47]. This statement seems odd given that the massless scalar wave equation is separable in the background of a 3 dimensional torus. Below we reproduce the computation for the separations of variables for the scalar wave equation in $d = 3$ dimensions as per [48]. Following this, we extend this approach to 4 dimensions and attempt to do the same in 5 dimensions.

We start with the metric in [48]. This metric is expressed as a $d = 3$ coordinate system and the coordinates are labelled as (η, θ, ψ).

$$ds^2 = \frac{a^2}{(\cosh\eta - \cos\theta)^2}[d\eta^2 + d\theta^2 + \sinh^2\eta d\psi^2]. \tag{3.22}$$

Where $0 \leq \eta < +\infty, \quad -\pi < \theta \leq +\pi, \quad 0 \leq \psi < 2\pi$. The Laplacian associated with this metric then becomes,

$$\nabla^2\Phi(\eta,\theta,\psi) = \frac{(\cosh\eta - \cos\theta)^3}{a^2\sinh\eta}\left\{\frac{\partial}{\partial\eta}\Big(\frac{\sinh\eta}{\cosh\eta - \cos\theta}\frac{\partial\Phi}{\partial\eta}\Big) + \sinh\eta\frac{\partial}{\partial\theta}\Big(\frac{1}{\cosh\eta - \cos\theta}\frac{\partial\Phi}{\partial\theta}\Big)\right\}$$
$$+ \frac{(\cosh\eta - \cos\theta)^2}{a^2\sinh^2\eta}\frac{\partial^2\Phi}{\partial\psi^2}. \tag{3.23}$$

The ansatz in [48] suggests as a possible solution for (3.23) is of the form,

$$\Phi(\eta,\theta,\psi) = (\cosh\eta - \cos\theta)^{1/2}H(\eta)\Theta(\theta)\Psi(\psi). \tag{3.24}$$

The above ansatz then separates into the following ordinary differential equations(ODE);

$$(\eta - 1)^2\frac{d^2H}{d\eta^2} + 2\frac{dH}{d\eta} - \Big(\frac{q^2}{\eta^2 - 1} - p^2 + \frac{1}{4}\Big) = 0, \tag{3.25}$$

$$\frac{d^2\Theta}{d\theta^2} + p^2\Theta = 0, \tag{3.26}$$

$$\frac{d^2\Psi}{d\psi^2} + q^2\Psi = 0. \tag{3.27}$$

The solution to these differential equations are,

$$\begin{aligned} H &= A\mathcal{P}^q_{p-\frac{1}{2}}(\cosh(\eta)) + B\mathcal{L}^q_{p-\frac{1}{2}}(\cosh(\eta)), \\ \Theta &= A\sin(p\theta) + B\cos(p\theta), \\ \Psi &= A\sin(p\psi) + B\cos(p\psi). \end{aligned} \tag{3.28}$$

The functions $(\mathcal{P}^q_{p-\frac{1}{2}}(\cosh\eta), \mathcal{L}^q_{p-\frac{1}{2}}(\cosh\eta))$ are Legendre polynomials of the first and second kind respectively.

In the above, p and q are separation constants. The coordinates (η, θ, ψ) are related to the coordinates of the black ring of [43] by,

$$y = -\cosh\eta, \tag{3.29}$$

$$x = -\cos\theta. \tag{3.30}$$

Then the metric (3.23) can be expressed in the Emparan-Reall coordinates [43] by;

$$ds^2 = \frac{R^2}{(x-y)^2}\left[(y^2 - 1)d\psi^2 + \frac{dy^2}{y^2 - 1} + \frac{dx^2}{1 - x^2}\right] \tag{3.31}$$

As stated above this expression is separable using the ansatz,

$$\Phi(x,y,\theta) = (x - y)^{-1/2}X(x)Y(y)\Psi(\psi). \tag{3.32}$$

And the differential equations (3.25), (3.26), and (3.27) become,

$$(y^2-1)\frac{d^2Y}{dy^2}+2\frac{dY}{dy}+\Big(\frac{q^2}{y^2-1}+p^2-\frac{1}{4}\Big)Y=0, \tag{3.33}$$

$$\frac{d^2X}{dx^2}-p^2X=0, \tag{3.34}$$

$$\frac{d^2\Psi}{d\psi^2}-q^2\Psi=0. \tag{3.35}$$

The $d = 3$ toroidal system is then easily extended to $d = 4$ dimensions taking the form of,

$$ds^2=\frac{R^2}{(x-y)^2}\left[(y^2-1)d\psi^2+\frac{dy^2}{y^2-1}+\frac{dx^2}{1-x^2}+(1-x^2)d\phi^2\right]. \tag{3.36}$$

The separation ansatz for the $d = 4$ toroidal system then becomes,

$$\Phi(x,y,\theta,\phi)=(x-y)^{-1/2}X(x)Y(y)\Psi(\psi)\mathrm{P}(\phi). \tag{3.37}$$

And the ODE become,

$$(y^2-1)\frac{d^2Y}{dy^2}+2\frac{dY}{dy}-(p^2-q^2)Y=0, \tag{3.38}$$

$$-(x^2-1)\frac{d^2X}{dx^2}-2\frac{dX}{dx}+(r^2-s^2)X=0, \tag{3.39}$$

$$\frac{d^2\Psi}{d\psi^2}-q^2\Psi=0 \tag{3.40}$$

$$\frac{d^2P(\phi)}{d\phi^2}-s^2P(\phi)=0. \tag{3.41}$$

The solutions to the above ODE are,

$$\begin{aligned}
Y(y) &= A\mathcal{P}^q_{\frac{\sqrt{4p^2-4q^2+1}}{2}-\frac{1}{2}}+B\mathcal{L}^q_{\frac{4p^2-4q^2+1}{2}-\frac{1}{2}},\\
X(x) &= A\mathcal{P}^s_{\frac{\sqrt{4r^2-4s^2+1}}{2}-\frac{1}{2}}+B\mathcal{L}^s_{\frac{\sqrt{4r^2-4s^2+1}}{2}-\frac{1}{2}},\\
\Psi(\psi) &= Ae^{q\psi}-Be^{-q\psi},\\
P(\phi) &= Ae^{s\phi}+Be^{-s\phi}
\end{aligned} \tag{3.42}$$

Following the separation in four dimensions of space-time we attempted to apply the same technique to five spacetime dimensions. We had assumed that the time (t) could be compactified in the additional dimension and thus render the scalar wave equation associated with the Laplacian of the neutral black ring solution separable. Alas, this was not the case. The wave equation proved not separable using the approach of [48]. This suggest that there might be some merit to the statement that the scalar wave equation of the neutral black ring might not be separable. There has been some work done on the separability of black holes within string theory, most notably by [49] and it would be interesting to see if the techniques developed in [49, 50] can be applied to the separability problem within black rings.

Next we review five dimensional super-symmetric black ring and the double rotating black ring solution. We will focus on both black ring solution in our application of the hidden conformal symmetry technique to black ring solutions.

3.5 Super-symmetric black rings

We now briefly discuss the $U(1)^3$ super-symmetric black ring solution. We adopt the conventions of [51], specifically with regards to the charge (Q_i) and dipole moments (q_i). Our focus is on the metric and not the field strengths and the one-forms of [51]. The 5-d metric is given by

$$ds_5^2 = -(H_1H_2H_3)^{-2/3}(dt+\omega)^2 + (H_1H_2H_3)^{1/3}d\mathrm{x}_4^2 \tag{3.43}$$

where,

$$d\mathrm{x}_4^2 = \frac{R^2}{(x-y)^2}\Big[\frac{dy^2}{y^2-1} + (y^2-1)d\psi^2 + \frac{dx^2}{1-x^2} + (1-x^2)d\phi^2\Big], \tag{3.44}$$

and,

$$\begin{aligned} H_1 &= 1 + \frac{Q_1 - q_2q_3}{2R^2}(x-y) - \frac{q_2q_3}{4R^2}(x^2-y^2), \\ H_2 &= 1 + \frac{Q_2 - q_3q_1}{2R^2}(x-y) - \frac{q_3q_1}{4R^2}(x^2-y^2), \\ H_3 &= 1 + \frac{Q_3 - q_1q_2}{2R^2}(x-y) - \frac{q_1q_2}{4R^2}(x^2-y^2) \end{aligned} \tag{3.45}$$

The ω is a one-form related to the ring's angular momentum and is expressed as,

$$\omega = \omega_\psi d\psi + \omega_\phi d\phi. \tag{3.46}$$

And the expressions for the two angular momenta are;

$$\begin{aligned} \omega_\phi &= -\frac{(1-x^2)R}{2(x-y)^2}\Big[q_1Q_1 + q_2Q_2 + q_3Q_3 - q^3\Big(3 - \frac{y^2-1}{x-y} + \frac{1-x^2}{x-y}\Big)\Big] \\ \omega_\psi &= -(q_1+q_2+q_3)\frac{(y^2-1)(x-y)}{(y^2-1)+(x-y)^2+2(x-y)} - \frac{y^2-1}{4R^2}\Big[q_1Q_1 + q_2Q_2 + q_3Q_3 \\ &\quad - q^3\Big(3 - \frac{y^2-1}{x-y} + \frac{1-x^2}{x-y}\Big)\Big]. \end{aligned} \tag{3.47}$$

With q defined as,

$$q \equiv (q_1q_2q_3)^{1/3}. \tag{3.48}$$

The flat metric is the same as the flat metric associated with the neutral rotating black ring solution. The following is assumed with respect to the $Q_i s$,

$$Q_1 \geq q_2q_3, \qquad Q_2 \geq q_1q_3, \qquad Q_3 \geq q_1q_2. \tag{3.49}$$

This is to ensure that $H_i \geq 0$. Unlike in [52, 9] we have not taken the simplification,

$$Q_1 = Q_2 = Q_3 = Q, \qquad q_1 = q_2 = q_3 = q. \tag{3.50}$$

However, as it would be seen later, our results for the near horizon geometry are similar to those of [52, 9], with the only difference being the value of $L(Q_i, q_i)$ which appears on both approaches. The coordinates of this ring solution are the same as those of the neutral single rotating black ring discussed in 3.2 above and in detail in [43]; where,

$$-1 \leq x \leq 1, \qquad -\infty < y \leq -1, \qquad 0 \leq \phi, \psi \leq 2\pi. \tag{3.51}$$

The horizon as is the case of the neutral single rotating black ring of [43] is located at $y = -\infty$.

3.5.1 Near Horizon Limit

To arrive at the near horizon limit we follow the formalism of [52, 9]. The complete derivation of the near horizon geometry is contain in appendix C. Below we state the result contained in the aforementioned appendix and in [52, 9].

The near horizon limit of the metric is becomes;

$$ds^2 = q^2\Big(\frac{dr^2}{r^2} + \frac{L^2}{q^2}d\psi^2 + \frac{Lr}{p}dtd\psi\Big) + \frac{q^2}{4}\big(d\theta^2 + \sin^2\theta d\phi^2\big) \tag{3.52}$$

In the derivation in appendix C, we did not make the simplifying assumption 3.50, however one can see that the near horizon metric (3.52) is very similar to that of [53, 52, 9] with the only difference being the definition of L. The definition for L is provided in appendix C.

The metric 3.52 will form the basis for our computation of the massless scalar wave equation using the Laplacian in the next section. This will ultimately lead us to the identification of the conformal symmetry associated with this black ring solution.

3.6 Double Rotating Black Ring

We now turn our attention to the neutral double rotating black ring (DRBR) solution discovered by Pomeransky et al [45]. The DRBR is a black ring solution with rotation in two directions, the ψ and $t\phi$ direction. The metric takes the form of;

$$\begin{aligned} ds^2 = &\frac{H(\hat{y},x)}{H(x,\hat{y})}(d\hat{t} + \Omega(x,\hat{y}))^2 - \frac{F(x,\hat{y})}{H(\hat{y},x)}d\psi - 2\frac{J(x,\hat{y})}{H(\hat{y},x)}d\phi d\psi \\ &+ \frac{F(\hat{y},x)}{H(\hat{y},x)}d\phi^2 + \frac{2k^2H(x,\hat{y})}{(x-\hat{y})^2(1-\nu)^2}\Big(\frac{dx^2}{G(x)} - \frac{d\hat{y}^2}{G(\hat{y})}\Big). \end{aligned} \tag{3.53}$$

Like the neutral singly rotating black ring, the ranges of the coordinates are, $-1 \leq x \leq 1$, $-\infty \leq \hat{y} \leq -1$ and $\phi, \psi \in [0, 2\pi]$. Similarly, for the DRBR solution, the S^1 is parametrised by ψ, and the S^2 is parametrised by (ϕ, θ). The functions contained (3.53) are defined as;

$$\begin{aligned} G(x) &= (1-x^2)(1+\lambda x+\nu x^2), \\ H(x,\hat{y}) &= 1+\lambda^2-\nu^2+2\lambda\nu(1-x^2)\hat{y}+2x\lambda(1-\hat{y}^2\nu^2)+x^2\hat{y}^2\nu(1-\lambda^2-\nu^2), \\ \Omega(x,\hat{y}) &= \frac{-2k\lambda((1+\nu)^2-\lambda^2)^{\frac{1}{2}}}{H(\hat{y},x)}(\nu^{\frac{1}{2}}\hat{y}(1-x^2)d\phi \\ &+ \frac{1+\hat{y}}{1+\lambda+\nu}(1+\lambda-\nu+\nu(1-\lambda-\nu)\hat{y}x^2+2\nu x(1-\hat{y}))d\psi), \\ J(x,\hat{y}) &= \frac{2k^2(1-x^2)(1-\hat{y}^2)\lambda\nu^{\frac{1}{2}}}{(x-\hat{y})(1-\nu)^2}(1+\lambda^2-nu^2+2(x-\hat{y})\lambda\nu-x\hat{y}\nu(1-\lambda^2-\nu^2)), \\ F(x,\hat{y}) &= \frac{2k^2}{(x-\hat{y})^2(1-\nu)^2}\Big(G(x)(1-\hat{y}^2)(((1-\nu)^2-\lambda^2)(1+\nu)+\hat{y}\lambda(1-\lambda^2+2\nu-3\nu^2)) \\ &+ G(\hat{y})(2\lambda^2+x\lambda(1-\nu)^2+\lambda^2)+x^2((1-\nu)^2-\lambda^2)(1+\nu) \\ &+ x^3\lambda(1-\lambda^2-3\nu^2+2\nu^3)-x^4(1-\nu)\nu(\lambda^2+\nu^2-1)\Big) \end{aligned} \tag{3.54}$$

This black ring solution is parametrised by k, λ and ν. Like the neutral singly rotating black ring, λ, ν are dimensionless and k has the dimension of length. These parameters have the following ranges;

$$k > 0, \quad 0 \leq \nu \leq 1, \quad 2\sqrt{\nu} \leq \lambda \leq 1 + \nu \tag{3.55}$$

The event horizon of the ring is worked out from the roots of $G(\hat{y})$ and we take the larger root,

$$y_h = \frac{-\lambda + \sqrt{\lambda^2 - 4\nu}}{2\nu} \tag{3.56}$$

3.6.1 Extremal DRBR solution

The extremal DRBR occurs when $\nu = \frac{\lambda^2}{4}$. The near horizon geometry of the extremal ring is determined by performing the following coordinate transformation [54];

$$\hat{y} \to \frac{-2}{\lambda} + \epsilon r, \quad \hat{t} \to \frac{16k}{(\lambda - 2)^2} \frac{t}{\epsilon}, \quad \hat{\phi} \to \phi + \frac{(\lambda - 2)(\lambda^2 + 4)}{8\lambda k(\lambda + 2)} \hat{t}, \quad \hat{\psi} \to \psi + \frac{(\lambda - 2)}{2k(\lambda + 2)} \hat{t}, \tag{3.57}$$

and taking the limit $\epsilon \to 0$. The resulting metric is,

$$\begin{aligned} ds^2 = & \frac{16k^2\Gamma(x)}{(\lambda - 2)^2} \Big(- r^2 dt^2 + \frac{dr^2}{r^2} \Big) + \frac{8\lambda^2 k^2 H(x)}{(\lambda x + 2)^4 (1 - x^2)(4 - \lambda^2)} dx^2 \\ & + 4 \frac{k^2 (2 + \lambda)^2}{(2 - \lambda)^2} d\psi^2 + \frac{32\lambda^2 k^2 (1 - x^2)}{H(x)(4 - \lambda^2)} (d\phi - r dt + \frac{4 + 8\lambda + \lambda^2}{4\lambda} d\psi)^2, \end{aligned} \tag{3.58}$$

with the functions $H(x)$ and $\Gamma(x)$ defined as,

$$H(x) = (\lambda^2 + 4)(1 + x^2) + 8\lambda x, \quad \Gamma(x) = \frac{\lambda^2 H(x)}{2(2 + \lambda x)^2 (2 + \lambda)^2}. \tag{3.59}$$

For the DRBR we will use the metric (3.58) in working out the Laplacian and eventually arrive at identifying the hidden conformal symmetries associated with this ring.

4

Black Ring - Hidden Conformal Symmetry

The conformal coordinates discussed in [42] and in chapter 2 were those of the non-extremal Kerr black hole. These conformal coordinates are not applicable to the extreme Kerr geometry which formed the basis of the original Kerr/CFT correspondence formulation by the authors of [6]. This can be seen from the conformal coordinate transformation we presented and discussed in 2.2.1.

$$\begin{aligned} \omega^{+} &= \sqrt{\frac{r-r_{+}}{r-r_{-}}}e^{2\pi T_R \phi} \\ \omega^{-} &= \sqrt{\frac{r-r_{+}}{r-r_{-}}}e^{2\pi T_L \phi - \frac{t}{2M}} \\ y &= \sqrt{\frac{r_{+}-r_{-}}{r-r_{-}}}e^{\pi(T_L+T_R)\phi - \frac{t}{4M}} \end{aligned} \tag{4.1}$$

When $r_{+} = r_{-}$, it is clear that these coordinates become meaningless. As we were studying extremal black rings, it was necessary to find a conformal coordinate transformation which is consistent with the extreme Kerr geometry. This, in our view was consistent with the argument and the derivation of the original Kerr/CFT correspondence by [6]. The conformal coordinate transformation consistent with the hidden conformal symmetry of the extreme Kerr geometry was presented by Chen et al in [55]. In their work [55], they applied the conformal coordinates to a number of extreme black holes. Some of the examples included in [55] are;

- Hidden conformal symmetry of extreme Kerr-Newman black hole,
- Hidden conformal symmetry of extreme Kerr in $d = 4$ dimensions, and,
- Extreme warped AdS_3 black hole.

In a different paper [56], they show that the conformal coordinates used in [55] to determine the hidden conformal symmetry of $d = 4$ extreme Kerr geometry could be extended to $d = 5$ spacetime. In [56] they successfully apply this approach to the 5D Kerr black hole.

As one can expect our analysis of the hidden conformal symmetry of both the supersymmetric black ring and the DRBR follows the work of [55] and to a lesser extent [42]. The approach we took for the black rings began with working out the massless wave equation using the Laplacian. Then we applied the conformal coordinate transformation of [56] to determine the quadratic

Casimir. We then compared the two to see if we could draw any conclusions between radial equation of the Laplacian and the quadratic Casimir.

4.1 Black ring Massless Scalar Wave Equation

4.1.1 Supersymmetric Black Ring

We begin this section by re-stating the near horizon limit of the $U(1)^3$ supersymmetric black ring solution as stated in 3.5.1 and [53, 9, 52].

$$ds^2 = q^2\left(\frac{dr^2}{r^2} + \frac{L^2}{q^2}d\psi^2 + \frac{Lr}{q}dtd\psi\right) + \frac{q^2}{4}\left(d\theta^2 + \sin^2\theta d\phi^2\right) \tag{4.2}$$

Following the approach of [42] we worked out the Klein-Gordon equation for the massless scalar wave equation associated with the above metric. The Klein-Gordon equation for the massless scalar is given by;

$$\frac{1}{\sqrt{-g}}\partial_\mu\left(\sqrt{-g}g^{\mu\nu}\partial_\nu\Phi\right) = 0 \tag{4.3}$$

We tried an ansatz similar to that of [42] as a solution to the Klein-Gordon equation above,

$$\Phi(t, r, \theta, \phi, \psi) = e^{-i\omega t + im\phi + in\psi}\Phi(r, \theta) \tag{4.4}$$

As the black ring solution is in $d = 5$ space-time, we have introduced ψ, the angle parametrising the S^1 of the black ring. Similar to the ϕ which parametrises S^2 in the Kerr solution, it is periodic in $\psi \sim \psi + 2\pi$. Furthermore, $\Phi(r, \theta)$ can be separated into the radial and the angular part and we have;

$$\Phi(r, t, \theta, \phi, \psi) = e^{-i\omega t + im\phi + in\psi}R(r)S(\theta) \tag{4.5}$$

The radial equation can be expressed as;

$$r^2\partial_r^2 R(r) + 2r\partial_r R(r) + \frac{m\omega q}{Lr}R(r) + \frac{\omega^2}{r^2}R(r) = K_\ell R(r) \tag{4.6}$$

In these coordinates the supersymmetric black ring has an event horizon at $r = 0$, hence we have not included the term $(r - r_+)$ as is the case in [42], where the event horizon is at some distance from $r = 0$.
The angular equation of the Laplacian can be expressed as;

$$\Big[\frac{1}{\sin\theta}\partial_\theta(\sin\theta\partial_\theta) + \frac{m\omega}{L\cos\theta} - \frac{n^2}{q^2(1-\cos^3\theta)}\Big]S(\theta) = -K_\ell S(\theta) \tag{4.7}$$

In both the radial and the angular equation, K_ℓ is the separation constant.

4.1.2 Double Rotating Black Ring

We follow the same process as in the previous section 4.1.1 in working out the hidden conformal symmetry of the DRBR solution. We restate the metric for the near horizon extremal limit of the DRBR we discussed in chapter 3

$$ds^2 = \frac{16k^2\Gamma(x)}{(\lambda-2)^2}\Big(-r^2dt^2+\frac{dr^2}{r^2}\Big)+\frac{8\lambda^2k^2H(x)}{(\lambda x+2)^4(1-x^2)(4-\lambda^2)}dx^2$$
$$+4\frac{k^2(2+\lambda)^2}{(2-\lambda)^2}d\psi^2+\frac{32\lambda^2k^2(1-x^2)}{H(x)(4-\lambda^2)}(d\phi-rdt+\frac{4+8\lambda+\lambda^2}{4\lambda}d\psi)^2, \tag{4.8}$$

with the functions $H(x)$ and $F(x)$ defined in (3.59).

We start by applying the Laplacian operator (4.3) to the metric (4.8) and we try the ansatz,

$$\Phi(r,x,t,\phi,\psi) = \Phi(r,x)e^{-i\omega t+im\phi+in\psi}, \tag{4.9}$$

as a solution to the Laplacian. The $\Phi(r,x)$ function can be further separated into the radial(r) and x equations of the Laplacian. As in the above section for the supersymmetric black ring 4.1.1 we have,

$$\Phi(r,x,t,\phi,\psi) = e^{-i\omega t+im\phi+in\psi}R(r)X(x). \tag{4.10}$$

Our interest is on the radial equation. The radial part then takes the form of,

$$\partial_r((r^2)\partial_r)R(r)+(\frac{\omega^2}{r^2}-\frac{m\omega}{r}) = K_\ell R(r). \tag{4.11}$$

Again K_ℓ is the separation constant.

4.2 Conformal Coordinates

Unlike in [42], where their analysis of hidden conformal coordinates focused on the near region of the Kerr solution (as discussed in 2.2), our analysis is limited to the extremal region of black rings. To this end, we use the conformal coordinates applicable to extremal black holes defined in [56]. The coordinates are defined as;

$$\begin{aligned}\omega^+ &= \frac{1}{2}\Big(\alpha_1 t+\beta_1\phi-\frac{\gamma_1}{r-r_+}\Big),\\ \omega^- &= \frac{1}{2}\Big(e^{2\pi T_L\phi+2n_Lt}\Big),\\ y &= \sqrt{\frac{\gamma_1}{2(r-r_+)}}e^{\pi T_L\phi+n_Lt}.\end{aligned} \tag{4.12}$$

Using this coordinate system, the vector fields which eventually lead to the quadratic Casimir are defined as;

$$\begin{aligned}H_1 &= i\partial_+\\ H_0 &= i\Big(\omega^+\partial_++\frac{1}{2}y\partial_y\Big)\\ H_{-1} &= i(\omega^{+2}\partial_++\omega_+y\partial_y-y^2\partial_-)\end{aligned} \tag{4.13}$$

and,

$$\begin{aligned}\bar{H}_1 &= i\partial_- \\ \bar{H}_0 &= i\Big(\omega^- \partial_- + \frac{1}{2} y\partial_y\Big) \\ \bar{H}_{-1} &= i(\omega^{-2}\partial_- + \omega_- y\partial_y - y^2\partial_+).\end{aligned} \tag{4.14}$$

The vector fields in (r, ϕ, t) coordinates are provided in appendix D. These vector fields obey the following $SL(2, \mathbb{R})$ Lie algebra.

$$\begin{aligned}[H_0, H_{\pm 1}] &= \mp i H_{\pm 1}, \\ [H_{-1}, H_1] &= -2iH_0.\end{aligned} \tag{4.15}$$

The above algebra also holds for $(\bar{H}_0, \bar{H}_{\pm 1})$. We will show later that these vector fields reduce to vectors very similar to the Killing vectors of [53] for the $U(1)^3$ supersymmetric black ring. In the next section we briefly discuss the quadratic Casimir associated with these vector fields.

4.3 Quadratic Casimir

The quadratic Casimir for these vector fields is

$$\begin{aligned}\mathcal{H}^2 = \bar{\mathcal{H}}^2 &= -H_0^2 + \frac{1}{2}(H_1 H_{-1} + H_{-1} H_1) \\ &= \frac{1}{4}(y^2\partial_y^2 - y\partial_y) + y^2\partial_+\partial_-\end{aligned} \tag{4.16}$$

The Casimir in (r, ϕ, t) coordinates is given by the expression;

$$\mathcal{H}^2 = \partial_r(\Delta\partial_r) - \Big(\frac{\gamma_1(2\pi T_L\partial_t - 2n_L\partial\phi)}{A(r - r_+)}\Big)^2 - \frac{2\gamma_1(2\pi T_L\partial_t - 2n_L\partial\phi)}{(r - r_+)A^2}(\beta_1\partial_t - \alpha_1\partial_\phi) \tag{4.17}$$

with A and Δ defined as,

$$\begin{aligned}A &= 2\pi T_L\alpha_1 - 2n_L\beta_1 \\ \Delta &= (r - r_+)^2\end{aligned} \tag{4.18}$$

4.3.1 Supersymmetric Black Ring

From the radial equation of the Laplacian of the $U(1)^3$ supersymmetric black ring we were able to express the above Casimir as;

$$\partial_r\Big(\Delta\partial_r\Big)R(r) + \Big(\frac{mq\omega}{Lr} + \frac{\omega^2}{r^2}\Big)R(r) = K_\ell R(r) \tag{4.19}$$

This we were able to achieve by setting the following constants to be,

$$\beta_1 = 0, \qquad \gamma_1 = \alpha_1 = 1, \qquad n_L = 0, \qquad T_L = \frac{L}{\pi q} \tag{4.20}$$

This recasting of left hand side of (4.19) into (4.17) is reminiscent of the NHEK analysis in [56].

4.3.2 DRBR

From (4.11) we were able to show that the Casimir associated with the DRBR solution is,

$$\partial_r(r^2)\partial_r R(r) + (\frac{\omega^2}{r^2} - \frac{m\omega}{r}) = K_\ell R(r). \tag{4.21}$$

From the above it then becomes easy to cast (4.11) into the same format as (4.17). This again is achieved by setting the following constants of equation (4.17) to be,

$$\beta_1 = n_L = 0, \quad \gamma_1 = \alpha_1 = 1, \quad T_L = \frac{1}{2\pi}. \tag{4.22}$$

4.4 Killing vectors and the SL(2)R algebra

As stated in [55, 56] the vector fields which generate (4.17) satisfy the $SL(2,\mathbb{R})$ algebra. Below we present the vector fields specifically for the $U(1)^3$ supersymmetric black ring solution.

$$\begin{aligned}
H_1 &= 2i\partial_t, \qquad H_0 = i(t\partial_t - r\partial_r), \\
\bar{H}_0 &= iq\partial_\phi, \qquad H_{-1} = i((r^{-2} + \frac{1}{2}t^2)\partial_r - \frac{q}{2Lr}\partial_\phi - rt\partial_r), \\
\bar{H}_1 &= -2ie^{\frac{-2L\phi}{q}}\big(\frac{1}{L}\partial_t - \frac{q}{L}\partial_\phi - r\partial_r\big), \\
\bar{H}_{-1} &= -i\frac{1}{2}e^{\frac{2L\phi}{q}}\big(\frac{1}{r}\partial_t - \frac{q}{2L}\partial_\phi + r\partial_r\big).
\end{aligned} \tag{4.23}$$

The vector fields satisfy the following $SL(2,\mathbb{R})$ algebra;

$$\begin{aligned}
&[H_0, H_1] = -iH_1, \qquad [H_0, H_{-1}] = iH_{-1}, \qquad [H_{-1}, H_1] = -2iH_0, \\
&[\bar{H}_0, \bar{H}_1] = -i\bar{H}_1, \qquad [\bar{H}_0, \bar{H}_{-1}] = i\bar{H}_{-1}, \qquad [\bar{H}_{-1}, \bar{H}_1] = -2i\bar{H}_0.
\end{aligned} \tag{4.24}$$

In the next section we use our results for temperature (T_L) to compute the microscopic entropy for both the black ring solutions respectively. This will be done through the application of the Cardy formula. This is then compared to the expressions for microscopic entropy obtained through other approaches.

5

CFT Interpretation

The focus of this chapter is on confirming the validity of the result for the left moving temperatures computed using the hidden conformal symmetry approach in the previous chapter 4. The temperature is used as input into the Cardy formula to work out the microscopic entropy. The expression for the microscopic entropy is then compared to those obtained through the ASG formalism or the Bekenstein-Hawking approach. This is done for both black ring solutions. Lastly, we compare the expressions for the microscopic entropy of the DRBR solution to that of the 5D extremal Myers-Perry black hole.

5.1 Entropy and CFT Interpretation: supersymmetric black ring

5.1.1 Bekenstein-Hawking Entropy

The Bekenstein-Hawking formula in $d = 5$ spacetime takes the form of [24];

$$S_{BH} = \frac{\mathcal{A}}{4G_5}, \tag{5.1}$$

$\mathcal{A}$ is the area of the event horizon, G_5 is the Newton gravitational constant in five dimensions. The spatial-cross section of the event horizon is given by [9],

$$ds^2_{horizon} = L^2 d\psi'^2 + \frac{q^2}{4}(d\theta^2 + \sin^2\theta d\chi^2). \tag{5.2}$$

In these coordinates one can see that the event horizon has an $S^1 \times S^2$ topology. The radius of the circle, S^1, is L^2 and of the two-sphere, S^2, is $q^2/4$ [9]. From here it is easy to compute the area of the event horizon. And it is given by,

$$\mathcal{A} = \int \sqrt{g_{\psi'\psi'} g_{\theta\theta} g_{\chi\chi}} d\theta d\chi d\psi'. \tag{5.3}$$

Using (5.2) as input into (5.3) we have,

$$\mathcal{A} = \frac{Lq^2}{4} \int_0^{2\pi} d\psi' \int_0^{2\pi} d\chi \int_0^{\pi} \sin\theta d\theta. \tag{5.4}$$

The ranges of the coordinates are; $\psi', \chi \in [0, 2\pi]$ and $\theta \in [0, \pi]$. We then have the value of the area as [9],

$$\mathcal{A} = 2\pi^2 L q^2. \tag{5.5}$$

The definition of q and L are provided in (3.48) and (C.8) respectively. Using the above expression for the area as input into the (5.1), we have the value of the microscopic entropy calculated from the horizon as in [43],

$$S_{BH} = \frac{\pi^2 L q^2}{2G_5}. \tag{5.6}$$

In the next section we look at the result we found for the left moving temperature with the intention of working out the entropy.

5.1.2 $U(1)^3$ supersymmetric black ring CFT Interpretation

In the previous chapter we determined the left moving temperature (T_L) by employing the hidden conformal symmetry approach. We found T_L to be,

$$T_L = \frac{L}{\pi q}. \tag{5.7}$$

Our goal is to use the Cardy formula to determine the macroscopic entropy. In order to do this, we need the value of the central charge associated with supersymmetric black ring. We will not reproduce it here, we will merely state it as in [57, 51],

$$c_L = \frac{3\pi q_1 q_2 q_3}{2G}. \tag{5.8}$$

The Cardy formula is given by,

$$S_C = \frac{\pi^2}{3} c_L T_L. \tag{5.9}$$

Now taking the value of the central charge (5.8) and using it as input into the Cardy formula (5.9) we find that our result reproduces the microscopic entropy determined using (5.6), i.e.

$$S_{BH} = S_C = \frac{\pi^2 L q^2}{2G_5}. \tag{5.10}$$

5.2 DRBR CFT Interpretation

The entropy and the Hawking temperature for the non-extremal DRBR solution are given by,

$$\begin{aligned} S_{BH} &= \frac{A}{4G_5} = \frac{8\pi^2 k^3 \lambda(1+\nu+\lambda)}{G_5(1-\nu)^2(y_h^{-1} - y_h)}, \\ T_H &= \frac{(y_h^{-1} - y_h)(1-\nu)\sqrt{\lambda^2 - 4\nu}}{8\pi k \lambda(1+\nu+\lambda)}. \end{aligned} \tag{5.11}$$

In 4.3.2 we were able to work out the temperature of the extremal DRBR solution. In this section we use that result to work out the microscopic entropy associated with the extremal DRBR solution. To remind the reader, the temperature of the left moving sector of the DRBR solution was worked out in (4.22) as,

$$T_L = \frac{1}{2\pi}. \tag{5.12}$$

This is in agreement with the temperature determined using the asymptotic symmetry group in [47] and quoted in [54]. From here we can determine the entropy using the Cardy formula (5.9). The central charge associated with this black ring solution is given by,

$$c_L^{\phi} = 12 J_{\phi}. \tag{5.13}$$

The entropy is then shown to be [47, 54]

$$S_{Cardy} = \frac{\pi^2}{3} c_L^{\phi} T_L = 2\pi J_{\phi}. \tag{5.14}$$

Unlike the case of the 5D MP black hole we do not have a J_{ψ} picture. This follows from the result that; in the case of the DRBR solution, the extremal limit only occurs along the ϕ direction and not the ψ direction.

5.3 5D Extremal Black Holes: a comparison

Below we compare the result for the temperature and the entropy for the extremal double rotating black black ring (DRBR) solution to that of the 5D extremal Myers-Perry black hole. The discussion below is a reproduction of the discussion on hidden conformal symmetries of a 5D Kerr black hole from [56]. We start the comparison by stating the near horizon geometry of the Myers-Perry black hole. The 5D Myers-Perry metric is of the form;

$$\begin{aligned} ds^2 = & \frac{\Delta}{\rho^2}\Big(dt - a\sin^2\theta d\phi - b\cos^2\theta d\psi\Big)^2 + \frac{\rho^2 dr^2}{\Delta} + \rho^2 d\theta^2 + \frac{sin^2\theta}{\rho^2}\Big(adt - (r^2+a^2)d\theta\Big)^2 \\ & + \frac{\cos^2\theta}{\rho^2}\Big(bdt - (r^2+b^2)d\psi\Big)^2 + \frac{1}{r^2\rho^2}\Big(abdt - b(r^2+a^2)\sin^2 d\phi - a(r^2+b^2)\cos^2\theta d\psi\Big)^2, \end{aligned} \tag{5.15}$$

where a and b are two rotation parameters and,

$$\begin{aligned} \Delta &= \frac{1}{r^2}(r^2+a^2)(r^2+b^2) - 2M, \\ \rho^2 &= r^2 + a^2\cos^2\theta + b^2\sin^2\theta. \end{aligned} \tag{5.16}$$

The reader will recognise the above as the metric for the 5D Kerr black hole solution. Like in the case of the 4d Kerr black hole solution, the location of the horizon is determined by solving $\Delta = 0$ equation. It then follows that the inner and out horizon is located at,

$$r_{\pm} = \sqrt{M - \frac{a}{2} - \frac{b^2}{2} \pm \sqrt{(M - \frac{1}{2}(a-b)^2(M - \frac{1}{2}(a+b)^2))}} \tag{5.17}$$

The event horizon for the MP black hole is parametrised by $\theta \in [0, \pi/2]$ and $\phi, \psi \in [0, 2\pi]$ and its topology is S^3 [54].

The Hawking temperature, Bekenstein-Hawking entropy, angular momenta and angular velocities at the horizon of this black hole are given by,

$$T_H = \frac{r_+^4 - a^2b^2}{2\pi r_+(r_+^2+a^2)(r_+^2+b^2)}, \qquad S_{BH} = \frac{\pi^2(r_+^2+a^2)(r_+^2+b^2)}{2G_5 r_\pm},$$
$$J_\phi = \frac{\pi M a}{2G_5}, \quad J_\psi = \frac{\pi M b}{2G_5}, \quad \Omega_\phi = \frac{a}{r_+^2+a^2}, \quad \Omega_\psi = \frac{b}{r_+^2+b^2}. \tag{5.18}$$

5.3.1 Extremal MP black holes

The extremal MP black hole occurs when $T_H = 0$, this occurs when,

$$r_+^2 = r_-^2 = ab, \quad M = \frac{1}{2}(a+b)^2 \tag{5.19}$$

The Bekenstein-Hawking entropy for the extremal MP black hole is given by,

$$S_{BH} = \frac{\pi^2}{2G_5}\sqrt{ab}(a+b)^2. \tag{5.20}$$

The near horizon geometry of the MP black hole is found by performing the following coordinate transformation and taking the limit $\epsilon \to 0$.

$$t \to \frac{(a+b)^2}{4}\frac{\hat{t}}{\epsilon}, \quad r \to \sqrt{ab} + \epsilon\hat{r}, \quad \phi \to \hat{\phi} + \frac{t}{a+b}, \quad \psi \to \hat{\psi} + \frac{t}{a+b}, \tag{5.21}$$

while keeping the hatted coordinates fixed. The metric (5.15) becomes;

$$ds^2 = \rho^2(-\frac{\hat{r}}{4}d\hat{t}^2 + \frac{\hat{r}^2}{4\hat{r}^2}) + \rho^2 d\theta^2 + \frac{2M}{\rho^2}\Big[a^2\sin^2\theta(d\hat{\phi} + k_{\hat{\phi}}\hat{r}d\hat{t})^2 + b^2\cos^2\theta(d\hat{\psi} + k_{\hat{\psi}}\hat{r}d\hat{t})^2$$
$$+ ab(\sin^2\theta(d\hat{\phi} + k_{\hat{\phi}}\hat{r}d\hat{t}) + \cos^2\theta(d\hat{\psi} + k_{\hat{\psi}}\hat{r}d\hat{t}))^2\Big], \tag{5.22}$$

where the value of ρ has changed to,

$$\rho = ab + a^2\cos^2\theta + b^2\sin^2\theta. \tag{5.23}$$

And the $k_{\hat{\phi}}$ and $k_{\hat{\psi}}$ are defined as,

$$k_{\hat{\phi}} = \frac{1}{2}\sqrt{\frac{b}{a}}, \quad k_{\hat{\psi}} = \frac{1}{2}\sqrt{\frac{b}{a}}. \tag{5.24}$$

5.3.2 Hidden Conformal Symmetry of the 5d Myers-Perry black hole

The 5D MP black hole has what is commonly referred to as the ψ and ϕ pictures, associated with the central charges and temperatures of the two chiral CFT pictures. The DRBR black ring solution on the other hand, only has an extremal limit in the ϕ direction, and not in the ψ direction. Hence our analysis of the hidden conformal symmetry, we only focus on the ϕ picture.

For working out the hidden conformal symmetry for the 5d MP black hole, the authors of [56] use the same conformal coordinate transformation (4.13) we used in chapter 4 for supersymmetric black ring and the DRBR. Given that the hidden conformal symmetry of the MP black hole has both an inner and outer horizon, the quadratic Casimir was restated to reflect this. The Casimir in (t, r, ϕ) coordinates is;

$$\mathcal{H}^2 = \partial_r((r-r_+)^2\partial_r) - \frac{\gamma_1^2(2\pi T_L\partial_t - 2n_L\partial_\phi)^2}{A_2^2(r-r_+)^2} - \frac{\gamma_1(2\pi T_L\partial_t - 2n_L\partial_\phi)(\beta_1\partial_t - \alpha_1\partial_\phi)}{A_2^2(r-r_+)}, \quad (5.25)$$

with $|A_2| = 2\pi T_L\alpha_1 - 2n_L\beta_1$. The sign of A_2 is chosen to make to $\beta_1/A_2 > 0$.

The massless scalar field of the 5D MP black hole can be decomposed into the following;

$$\Phi(t, \phi, \psi, r, \theta) = R(r)S(\theta)e^{-i\omega t + im_\phi\phi + im_\psi\psi} = R(r)S(\theta)e^{-i\omega t + im_R(\phi+\psi) + im_L(\phi-\psi)}, \quad (5.26)$$

with $m_{\phi,\psi} = m_R \pm m_L$. The same process is followed as in chapter 4 in terms of finding the hidden conformal symmetry. After the separation of variables, the radial equation is,

$$\frac{\partial}{\partial x}\Big(x^2 - \frac{1}{4}\Big)\frac{\partial}{\partial x}R + \frac{1}{4}\Big[x\Delta\omega^2 - \Lambda + M\omega^2 + \frac{1}{x-\frac{1}{2}}\Big(\frac{\omega}{k_+} - \frac{m_R\Omega_R + m_L\Omega_L}{k_+}\Big) - \frac{1}{x+\frac{1}{2}}\Big(\frac{\omega}{k_-} - \frac{m_R\Omega_R - m_L\Omega_L}{k_+}\Big)\Big]R = 0. \quad (5.27)$$

The term Δ, is a constant which does not factor into computation and Λ is a representation for the eigenvalue of the angular Laplacian. And x is defined as,

$$x = \frac{r^2 - \frac{1}{2}(r_+^2 + r_-^2)}{r_+^2 - r_-^2}. \quad (5.28)$$

For the extremal limit, the radial equation becomes,

$$\frac{\partial}{\partial r^2}(r^2 + r_+^2)^2\frac{\partial}{\partial r^2}R(r) + \frac{ab(a+b)^4}{4(r^2+r_+^2)^2}\Big(\omega - \frac{m_\phi + m_\psi}{(a+b)^2}\Big)^2 R(r) + \frac{(a+b)^4}{4(r^2-r_+^2)}\Big[(\omega - \frac{(a-b)(m_\phi - m_\psi)}{(a+b)^2}\Big]R(r) = KR(r). \quad (5.29)$$

To proceed, another coordinate transformation is performed, $\phi' = \alpha\phi + \beta\psi$ and $\psi' = \gamma\phi + \delta\psi$. The angular coordinates then become linearly independent [56] . We have,

$$\begin{bmatrix} \alpha & \beta \\ \gamma & \delta \end{bmatrix} \in SL(2, \mathbb{Z}). \quad (5.30)$$

The expression $e^{im_\phi\phi + im_\psi\psi} = e^{im_{\phi'}\phi' + im_{\psi'}\psi'}$ lead to,

$$m_\phi = \alpha m_{\phi'} + \gamma m_{\psi'} = \beta m_{\phi'} + \delta m_{\psi'}. \quad (5.31)$$

To gain insight into the rotation on the ϕ' direction, [56] $m_{\psi'}$ is set to zero ($m_{\psi'} = 0$). The radial equation (5.29) becomes,

$$\partial_{r^2}(r^2 - r_+^2)^2\partial_{r^2}R(r) + \frac{ab(a+b)^4}{4(r^2-r_+^2)^2}\Big(\omega - \frac{(\alpha+\beta)m_{\phi'}}{a+b}\Big)^2 R(r) \frac{(a+b)^4}{4(r^2-r_+^2)}\Big(\omega - \frac{(\alpha+\beta)m_{\alpha'}}{a+b}\Big)\Big[\omega - \frac{(\alpha-\beta)(a-b)m_{\phi'}}{(a+b)^2}\Big]R(r) = KR(r). \quad (5.32)$$

We then set $m \to m_{\phi'}$ in (5.25) and we recover the equation for the quadratic Casimir [56]. And we can read off the following expression;

$$\begin{aligned} \beta_1^{\phi'} &= \frac{(a+b)^2}{(\alpha-\beta)(a-b)}\alpha_1^{\phi'}, \quad \gamma_1^{\phi'} = -\frac{-(\alpha b+\beta a)\sqrt{ab}(a+b)^2}{(\alpha-\beta)(a-b)}\alpha_{1,}^{\phi'}, \\ T_L^{\phi'} &= \frac{\sqrt{ab}}{\pi(\alpha b+\beta a)}, \quad n_L^{\phi'} = -\frac{(\alpha+\beta)\sqrt{ab}}{(\alpha b+\beta a)(a+b)}. \end{aligned} \tag{5.33}$$

Taking the value of the central charge for the extremal 5D Myers-Perry black hole,

$$c_L^{\phi'} = \frac{3\pi}{2}(\alpha b+\beta a)(a+b)^2, \tag{5.34}$$

and plugging into the Cardy formula, one finds that the entropy is the same as the Bekenstein-Hawking entropy,

$$S_{Cardy} = S_{BH} = \frac{\pi^2}{2G_5}\sqrt{ab}(a+b)^2. \tag{5.35}$$

5.3.3 Entropy Comparison

We now compare the value for the entropy of the extremal 5D MP black hole, to the value of the entropy for the extremal DRBR solution. We firstly need to simplify the expression for the MP black hole to ensure that we are comparing similar objects.

We start this process by remembering that the DRBR is parametrised by k, λ and, ν. At the extremal point we have $\nu = \frac{\lambda^2}{4}$. At the limit $\lambda \to 2$, both the MP black hole and the DRBR have the same mass and spin. To arrive at the point where we can compare the respective entropy expression, we focus at a point in the parameter space when $J_\psi = 3J_\phi$ [54]. At this limit, the entropy of the MP black (5.35) can be restated as,

$$\begin{aligned} S_{MP} &= \frac{\pi^2}{2G_5}\sqrt{ab}(a+b)^2, \\ &= \frac{\pi^2}{2G_5}\Big(\frac{2G_5}{\pi M}\sqrt{3J_\phi^2(2M)}\Big), \\ &= 2\pi\sqrt{3}J_\phi. \end{aligned} \tag{5.36}$$

Here we have used the relation $M = 1/2(a+b)^2$ and the relationship between J_ϕ and J_ψ for the MP black hole at extremality. We see that the entropy of the MP black hole is $\sqrt{3}$ greater than the entropy of the DRBR worked above (5.14) to be, $S_{DRBR} = 2\pi J_\phi$. The geometry with the larger entropy tends to be more stable, and in this case the MP black would be more stable than the DRBR solution. By studying the moduli space of 5D extremal black holes in the near horizon limit, the authors of [58] have shown that the entropy obtained through the Kerr/CFT conjecture is consistent with the Bekenstein-Hawking entropy.

In the next section we make a few remarks concerning the results of our analysis and suggest possible areas of future research and/or investigation as we conclude this report.

6

Concluding Remarks and Outlook

6.1 Concluding Remarks

We have successfully applied the conformal transformations of [55] to work out the hidden conformal symmetries of both a supersymmetric black ring and a non-supersymmetric double rotating black ring (DRBR) solution. We were able to show that in the near horizon region, both black ring solutions exhibited symmetries of the $SL(2,\mathbb{R})_L \times SL(2,\mathbb{R})_R$ group. However this symmetry was spontaneously broken when one moved towards the global geometry of the black ring solution. This was similar to the spontaneous symmetry breaking found by Strominger et al ([42]) in their analysis of the near region of Kerr black hole.

In both instances we were able to confirm our expression for the microscopic entropy with those obtained through other approaches, namely the macroscopic entropy using the Bekenstein-Hawking approach and the strong Kerr/CFT conjecture. Our focus was limited to the near horizon extremal regions of both black ring solutions. It would be interesting to investigate if these same conformal coordinates could be applied to regions away from the horizon, i.e. far from the horizon of extremal black rings and what sort of physics and symmetries could be observed in these regions.

Our work only looked at two classes of extremal black ring solutions, and attempted a 3rd, unsuccessfully (Elvang' extremal charged single rotating black ring analysed in [44]). It would be interesting to investigate the necessary and sufficient conditions which allow for the successful application of the conformal coordinate transformations we employed in our analysis. The assumption we made in our analysis, which proved insufficient, was that the black ring solution had to have an upper bound of the angular momentum, i.e. an extremal limit.

6.2 Outlook

Kerr/CFT is based on the Lie derivatives of the metric, one would expect to see different symmetries with the black ring given the difference in metrics. However that is not the result we found or the resulted in [53] which stated that the global symmetry of the near horizon of the $\mathcal{N} = 2$ supergravity is $U(1))_L \times SL(2)_R$. It would be useful to identify a mechanism to differentiate the symmetries of the near horizon extremal black ring geometry from those of the NHEK geometry.

The flat metric of the $5d$ black ring solution is separable and its been one of our questions in this research if one can arrive a point where the curved metric becomes separable as one approaching asymptotic infinity. What might warrant further investigation is; under what conditions can the curved metric be simplified to arrive at separability. Another approach which can be explored, is what are the necessary and sufficient conditions to have separability of the $5d$ black ring metric? The investigation of these conditions might follow the approach explored in [48] where the authors employ Stackel matrices.

In chapter 3 we briefly discussed the challenges with applying the separation of variables technique to the neutral singly rotating black ring solution. One of the ways this challenge can be circumvented is through the application of the black hole monodromy technique. This procedure developed to some detail in [59] rests on the assumption that the analytical properties of a solution are connected to the singular points of a wave equation at some specified boundary condition. The procedure involves the identification of a fundamental matrix for the ordinary differential equations (ODE), the monodromies at all branch points, and the local behaviour of Φ (a possible solution) around singular points [59].Through the application of this procedure, one can better understand the scattering coefficients and quasinormal modes in various black hole backgrounds. Furthermore, the elementary symmetries relevant to the extreme Kerr geometry were also identified using this technique in [59]. In [60] these techniques were successfully applied to the 5D Myers-Perry (MP) black hole solution to identify the left and the right moving temperatures. In the same paper, the hidden conformal symmetries of the 5D MP black hole were also worked-out using this technique. In [61] the techniques were successfully applied to the dipole and double rotating black role (DRBR). In future work it would be interesting to see if this technique can provide more insight into the scattering behaviour of the wave equation of the neutral black ring solution around singular points.

Over the past few years there's been research into how the black hole uniqueness theorems could be expanded to $d \geq 5$, spacetime. These ideas have largely been limited to supersymmetric black holes and black ring solutions in σ-models in $d = 5$ dimensions [62, 63]. The uniqueness theorem put forward in [63] for charged dipole rings in $d = 5$ dimensional minimal supergravity can be summarized as follows; a black ring in $d = 5$ Einstein-Maxwell-Chern-Simons theory with finite temperature can be uniquely characterized by its mass, electric charge, two independent angular momentum, dipole charge and the rod data. This rod data corresponds to the ratio of the S^2 radius to that of the S^1 radius. The result presented in [62] on the other hand can be summarised as; the only regular black ring solution with a regular event horizon is the $d = 5$ vacuum Pomeransky-Sen'kov (DRBR) ring with a constant mapping. This uniqueness theorem for the DRBR solution is constructed using a rotating self-gravitating σ-model. This raised interesting questions as to whether these ideas can be extended to the generic black ring solution (neutral single rotating black ring), and if they can, would there be a need to introduce an additional parameter over and above the asymptotic charges to describe the neutral black ring solution.

Appendix A

Conformal Group Generators and Algebra

In chapter 1 we briefly discussed the conformal group. In section 1.5.2 we stated that conformal transformations are a change of coordinates $\sigma^\mu \to \bar{\sigma}^\mu(\sigma)$. The metric tensor transforms as;

$$g_{\mu\nu}(\sigma) \to \Omega^2(\sigma) g_{\mu\nu}(\sigma). \tag{A.1}$$

This metric tensor is associated with a d dimensional spacetime. The conformal group is an extension of the Poincaré group. Over and above the translations and rotations associated with the Poincaré group, we also have dilation which scales the entire space and also special conformal transformation (SCT) [29].

The generators of the conformal group are given by,

$$\begin{aligned} \text{translation} \qquad & P_\mu = -i\partial_\mu, \\ \text{dilation} \qquad & D = -ix^\mu \partial_\mu, \\ \text{rotation} \qquad & L_{\mu\nu} = i(x_\mu \partial_\nu - x_\nu \partial_\mu,) \\ \text{SCT} \qquad & K_\mu = -i(2x_\mu x^\nu \partial_\nu - x^2 \partial_\mu). \end{aligned} \tag{A.2}$$

The algebra of the conformal group is,

$$\begin{aligned} [D, P_\mu] &= iP_\mu \\ [D, K_\mu] &= -iK_\mu \\ [K_\mu, P_\nu] &= 2i(\eta_{\mu\nu} D - L_{\mu\nu}) \\ [K_\rho, L_\mu] &= i(\eta_{\rho\mu} P_\nu - \eta_{\rho\nu} P_\mu K_\mu [P_\rho, L_{\mu\nu}] \\ &= i(\eta_{\rho\mu} P_\nu - \eta_{\rho\nu} P_\mu)[L_{\mu\nu}, L_{\rho\sigma}] \\ &= i(\eta_{\nu\rho} L_{\mu\sigma} + \eta_{\mu\sigma} L_{\nu\sigma} L_{\nu\rho} - \eta_{\mu\rho} L_{\nu\sigma} - \eta_{\nu\sigma} L_{\mu\rho}) \end{aligned} \tag{A.3}$$

Appendix B

$SL(2,\mathbb{R})$ Group

In this chapter we review properties of the $SL(2,\mathbb{R})$ group which render it useful to particle physics and conformal field theory.

B.1 Definition of the Group

The $SL(2,\mathbb{R})$ group is a Lie group of 2×2 matrices with real entries and det $= 1$, i.e $SL(2,\mathbb{R}) = \{A : A \quad \text{is} \quad \text{a} \quad 2\times 2 \quad \text{matrix,} \quad \text{with} \quad \det = 1\}$. The largest subgroup of the $SL(2,\mathbb{R})$ group is its centre $Z = \{\pm I\}$, where I is the identity matrix,

$$I = \begin{pmatrix} 1 & 0 \\ 0 & 1 \end{pmatrix}$$

The $SL(2,\mathbb{R})$ group is associated with Möbius or linear-fractional maps. These maps are [64]:

$$g : \chi \mapsto g \cdot \chi = \frac{a\chi + b}{c\chi + d}, \quad \text{where} \quad g = \begin{pmatrix} a & b \\ c & d \end{pmatrix}, \chi \in \mathbb{R} \tag{B.1}$$

The linear-fractional maps (B.1) are the left action of the $SL(2,\mathbb{R})$ group. This linear action induces a morphism of the projective line $P\mathbb{R}^1$ [65]. The action (B.1) also works as a map of complex numbers $z = \chi + iy$. If $y > 0$ then $g \cdot z$ has a positive imaginary part, i.e., (B.1) defines a map from the upper half-plane to itself [64].
The group $SL(2,\mathbb{R})$ acts on $\mathbb{R}^2$ by matrix multiplication on the column vectors,

$$\mathcal{L}_g : \begin{pmatrix} x_1 \\ x_2 \end{pmatrix} \mapsto \begin{pmatrix} ax_1 + bx_2 \\ cx_1 + dx_2 \end{pmatrix} = \begin{pmatrix} a & b \\ c & d \end{pmatrix} \begin{pmatrix} x_1 \\ x_2 \end{pmatrix}, \quad g = \begin{pmatrix} a & b \\ c & d \end{pmatrix} \in SL(2,\mathbb{R})$$

B.2 Lie Algebra

The $SL(2,\mathbb{R})$ group has a Lie algebra $\mathfrak{sl}_2(\mathbb{R})$ which is a set of of 2×2 matrices with zero trace i.e. $\mathfrak{sl}_2(\mathbb{R}) = \{A : A \quad \text{is} \quad \text{a} \quad 2\times 2 \quad \text{matrix,} \quad \text{with} \quad \text{tr}A = 0\}$ [66, 67]. The basis for the algebra, $\mathfrak{sl}_2(\mathbb{R})$ is,

$$X_+ = \begin{pmatrix} 0 & 1 \\ 0 & 0 \end{pmatrix} \qquad X_- = \begin{pmatrix} 0 & 0 \\ 1 & 0 \end{pmatrix} \qquad H = \begin{pmatrix} 1 & 0 \\ 0 & -1 \end{pmatrix}.$$

.

The complexification of the Lie algebra $\mathfrak{sl}_2(\mathbb{C})$ has the following basis,

$$E_+ = \begin{pmatrix} 1 & i \\ i & -1 \end{pmatrix} \qquad E_- = \begin{pmatrix} 1 & -i \\ -i & -1 \end{pmatrix} \qquad W = \begin{pmatrix} 0 & 1 \\ -1 & 0 \end{pmatrix}.$$

The commutators (eigen-relations) associated with this algebra are,

$$\begin{aligned} &[H, X_-] = 2X_+, && [H, X_-] = -2X_-, && [X_+, X_-] = H, \\ &[W, E_+] = -2iE_+, && [W, E_-] = -2iE_-, && [E_+, E_-] = -4iW \end{aligned} \tag{B.2}$$

B.3 The Quadratic Casimir

The element at the centre of the universal enveloping algebra $\mathfrak{U}(g)$ is the Casimir operator, defined as,

$$\omega = H^2 + 2(X_+X_- + X_-X_+). \tag{B.3}$$

The Casimir operator ω commutes with all H, X_+, X_-, it therefore lies at the centre of the algebra [66, 68]. We show that the Casimir commutes with all the generators of the group,

$$\begin{aligned} [H, \omega] &= H(H^2 + 2(X_+X_- + X_-X_+)) - (H^2 + 2(X_+X_- + X_-X_+))H \\ &= H^3 + 2HX_+X_- + 2HX_-X_+ - H^3 - 2X_+X_-H - 2X_-X_+H \\ &= 0. \end{aligned} \tag{B.4}$$

We also have,

$$\begin{aligned} [X_+, \omega] &= X_+(H^2 + 2(X_+X_- + X_-X_+)) - (H^2 + 2(X_+X_- + X_-X_+))X_+ \\ &= X_+H^2 + 2X_+^2X_- + 2X_+X_-X_+ - H^2X_+ - 2X_+X_-X_+ - 2X_-X_+^2 \\ &= 0. \end{aligned} \tag{B.5}$$

Lastly we have,

$$\begin{aligned} [X_-, \omega] &= X_-(H^2 + 2(X_+X_- + X_-X_+)) - (H^2 + 2(X_+X_- + X_-X_+))X_- \\ &= X_-H^2 + 2X_-X_+X_- + 2X_-^2X_+ - H^2X_- - 2X_+X_-^2 - 2X_-X_+X_- \\ &= 0 \end{aligned} \tag{B.6}$$

B.4 $SL(2, \mathbb{R})$ and AdS_3

Next we briefly discuss the $SL(2, \mathbb{R})$ in the context of AdS_3 spacetime. The discussion will be done using The Poincaré coordinates. AdS_3 can be viewed as a hyperboloid described by $-U^2 - V^2 + X^2 + Y^2 = -l^2$ embedded in a space with a metric,

$$ds^2 = -dU^2 - dV^2 + dX^2 + dY^2. \tag{B.7}$$

l is the radius of curvature of AdS_3. The Poincaré coordinates are,

$$U = \frac{1}{2r}(l^2 + x^2 + r^2 - t^2), \qquad V = l\frac{t}{r} \tag{B.8}$$

$$Y = \frac{-1}{2r}(l^2 + x^2 + r^2 - t^2), \qquad X = l\frac{x}{r} \tag{B.9}$$

In these coordinates the metric then becomes,

$$ds^2 = (l^2/r^2)(-dt^2 + dx^2 + dr^2). \tag{B.10}$$

The ranges of the coordinates t, x and r are $t, x \in (-\infty, \infty)$ and $r \in [0, \infty]$. The boundary is at $r = 0$ and the an event horizon at $r = \infty$. The Poincaré coordinates do not cover the entire AdS_3 only half of the space [33].

Before stating the generators of the $SL(2, \mathbb{R})$ within on AdS_3, we state the generators of the $SO(2, 2)$ group which is isometric to the $SL(2, \mathbb{R})$ group. We have,

$$\begin{aligned}
&[J_{01}, J_{02}] = J_{12} \quad [J_{01}, J_{03}] = -J_{23} \quad [J_{01}, J_{03}] = -J_{13} \quad [J_{02}, J_{12}] = J_{01} \\
&[J_{01}, J_{12}] = J_{02} \quad [J_{02}, J_{23}] = -J_{03} \quad [J_{01}, J_{13}] = J_{03} \quad [J_{03}, J_{13}] = J_{01} \\
&[J_{03}, J_{23}] = J_{02} \quad [J_{12}, J_{13}] = J_{23} \quad [J_{12}, J_{23}] = -J_{13} \quad [J_{13}, J_{23}] = J_{12}.
\end{aligned} \tag{B.11}$$

We have J_{ab} defined as,

$$J_{ab} = x_b \frac{\partial}{\partial x^a} - x_a \frac{\partial}{\partial x^b}, \tag{B.12}$$

where $x^a = (U, V, X, Y)$. [69]. This allow us to redefine the generators of $SL(2, \mathbb{R})$ as,

$$\begin{aligned}
SL(2, \mathbb{R})_L &= \{L_1 = (J_{01} + J_{23})/2, \quad L_2 = (J_{02} - J_{13})/2, \quad L_3 = (J_{12} + J_{03})/2\} \\
SL(2, \mathbb{R})_R &= \{\bar{L_1} = (J_{01 - J_{23}})/2, \quad \bar{L_2} = (J_{02} + J_{13})/2, \quad \bar{L_3} = (J_{01} - J_{03})\}.
\end{aligned} \tag{B.13}$$

The commutator relations are;

$$[L_1, L_2] = -L_3 \quad [L_1, L_3] = L_2, \quad [L_2, L_3] = L_1 \tag{B.14}$$

These also hold true for $\bar{L}$. A linear combination of these generators enable us to construct the algebra of $SL(2, \mathbb{R})$. The algebra takes the familiar form of,

$$[L_0, L_\pm] = \mp L_\pm \quad [L_+, L_-] = 2L_0. \tag{B.15}$$

The basis forming the algebra (B.15) relates to the elements of the generator (B.13) as,

$$L_0 = -L_2, \quad L_+ = i(L_1 + L_3), \quad L_- = i(L_i - L_3) \tag{B.16}$$

We can also express elements of this basis (B.15) in Poincaré coordinates (B.9) by employing (B.12). Firstly we introduce a coordinate transformation, $z = x + t$ and $\bar{z} = t - x$. Then the basis takes the form of,

$$\begin{aligned}
L_0 &= -\frac{r}{2}\partial_r - z\partial_z \\
L_- &= il\partial_z \\
L_+ &= -\frac{i}{l}[zr\partial_r + z^2\partial_z + r^2\partial_{\bar{z}}]
\end{aligned} \tag{B.17}$$

And the $\bar{L}$ part we have,

$$\begin{aligned}\bar{L}_0 &= -\frac{r}{2}\partial_r - \bar{z}\partial_{\bar{z}} \\ \bar{L}_- &= il\partial_{\bar{z}} \\ \bar{L}_+ &= -\frac{i}{l}[\bar{z}r\partial_r + z^2\partial_{\bar{z}} + r^2\partial_z]\end{aligned} \tag{B.18}$$

And now we can express the quadratic Casimir using this basis as,

$$\begin{aligned}L^2 &= \frac{1}{2}(L_+L_- + L_-L_+) - L_0^2 \\ &= \frac{1}{4}\Big(r^2\partial_r^2 - r\partial_r\Big) - r^2\partial_z\partial_{\bar{z}}.\end{aligned} \tag{B.19}$$

Appendix C

Supersymmetric Black Ring near horizon geometry

In sec 3.5.1 we discussed the process of taking the near horizon limit of the $U(1)^3$ supersymmetric black ring. In this appendix we provide a bit more detail. To remind the reader, the metric is of the form;

$$ds^2 = -(H_1 H_2 H_3)^{-2/3}(dt+\omega)^2 + (H_1 H_2 H_3)^{1/3} dx_4^2, \tag{C.1}$$

where,

$$dx_4^2 = \frac{R^2}{(x-y)^2}\left[\frac{dy^2}{y^2-1} + (y^2-1)d\psi^2 + \frac{dx^2}{1-x^2} + (1-x^2)d\phi^2\right] \tag{C.2}$$

The definition of H_1, H_2 and H_3 are is provided in (3.45). To take the near horizon geometry it is best to work in coordinate r, defined as $r = -R/y$. To get to the near horizon, the following coordinate transformations become useful,

$$dt = dv - B(r)dr, \tag{C.3}$$

$$d\phi = d\phi' - C(r)dt, \tag{C.4}$$

$$d\psi = d\psi' - C(r)dr. \tag{C.5}$$

The functions $B(r)$ and $C(r)$ are defined as

$$B(r) = \frac{B_2}{r^2} + \frac{B_1}{r} + B_0, \tag{C.6}$$

$$C(r) = \frac{C_1}{r} + C_0, \tag{C.7}$$

where $B_2 = q^2 L/(4R)$ and $C_1 = -q/(2L)$. The expression for L is given as;

$$L \equiv \frac{1}{2q^2}\left[2\sum_{i<J} \mathcal{Q}_i q_i \mathcal{Q}_j q_j - \sum_i \mathcal{Q}_i^2 q_i^2 - 4R^2 q^3 \sum_i q_i\right]^{1/2} \tag{C.8}$$

where the $\mathcal{Q}_i$ are defined as,

$$\mathcal{Q}_1 = Q_1 - q_2 q_3, \qquad \mathcal{Q}_2 = Q_2 - q_3 q_1, \qquad \mathcal{Q}_3 = Q_3 - q_1 q_2. \tag{C.9}$$

And q was defined in 3.48 as,

$$q \equiv (q_1 q_2 q_3)^{1/3}. \tag{C.10}$$

Just as a side remark, in order to avoid the solution having closed timelike curves, the following inquality needs to hold;

$$2q^2L^2 \equiv 2\sum_{i<J} \mathcal{Q}_i q_i \mathcal{Q}_j q_j - \sum_i \mathcal{Q}_i^2 q_i^2 - 4R^2 q^3 \sum_i q_i \geq 0. \tag{C.11}$$

This is a necessary and sufficient condition for the supersymetric black ring solutions not to have closed timelike curve [51].

The definition of B_0, B_1 and C_0, is,

$$B_1 = \frac{(Q+2q^2)}{4L} + \frac{L(Q-q^2)}{3R^2}, \tag{C.12}$$

$$C_0 = -\frac{(Q-q^2)^3}{8q^3RL^3}, \tag{C.13}$$

$$B_0 = \frac{q^2L}{8R^3} + \frac{2L}{3R} + \frac{3R^3}{2L^3} + \frac{3(Q-q^2)^3}{16q^2RL^3}. \tag{C.14}$$

The metric C.1 then becomes,

$$\begin{aligned} ds^2 = &-\frac{16r^4}{q^4}dv^2 + \frac{2R}{L}dvdr + \frac{4r^3\sin^2\theta}{Rq}dvd\phi' + \frac{4Rr}{q}dvd\psi' \\ &+ \frac{3(q_1+q_2+q_3)r\sin^2\theta}{L}drd\phi' + 2\Big[\frac{Lq}{R}\cos\theta - c\Big]drd\psi' \\ &+ L^2d\psi'^2 + \frac{q^2}{4}\Big[d\theta^2 + \sin^2\theta(d\phi'+d\psi')^2\Big] + \ldots, \end{aligned} \tag{C.15}$$

where c is defined as,

$$c = \frac{1}{2LRq_1q_2q_3}\Big[\mathcal{Q}_1\mathcal{Q}_2\mathcal{Q}_3 - R^2\sum_{i<j}(\mathcal{Q}_i+\mathcal{Q}_j)q_iq_j - q^3(q_1+q_2+q_3)R^2\Big]. \tag{C.16}$$

The definition of $\mathcal{Q}_i$s is provided in (3.49). Also, we remind the reader that $\cos\theta = x$ as stated in (3.13). The next step is to take the near horizon limit using the following transformations in r.

$$r = \epsilon L\bar{r}/R, \quad v = \bar{v}/\epsilon, \quad \epsilon \to 0. \tag{C.17}$$

After taking the near horizon limit, the metric (C.15) becomes,

$$ds^2 = 2d\bar{v}d\bar{r} + \frac{4L}{q}\bar{r}d\bar{v}d\psi' + L^2d\psi'^2 + \frac{q^2}{4}(d\theta^2 + \sin^2\theta d\phi^2). \tag{C.18}$$

There are two more transformations one needs to perform to arrive at the near horizon metric. These are,

$$d\psi' = d\psi - \frac{q}{2L}\frac{d\bar{r}}{\bar{r}}, \tag{C.19}$$

$$d\bar{v} = dt + \frac{q^2}{4}\frac{d\bar{r}}{\bar{r}}. \tag{C.20}$$

The near horizon metric as per (3.5.1) is then,

$$ds^2 = q^2\Big(\frac{dr^2}{r^2} + \frac{L^2}{q^2}d\psi^2 + \frac{Lr}{p}dtd\psi\Big) + \frac{q^2}{4}\big(d\theta^2 + \sin^2\theta d\phi^2\big). \tag{C.21}$$

Appendix D

Hidden Conformal Symmetry vector fields in (r, ϕ, t) coordinates

Below we express vector fields, which are Killing vectors, in (4.14) and (4.15) in global coordinates.

$$
\begin{aligned}
H_1 &= i\frac{2}{A}(2\pi T_L\partial_t - 2n_L\partial_\phi) \\
H_0 &= i\Big(- (r-r_+)\partial_+ + \frac{1}{A}(\alpha_1 t + \beta_1\phi)(2\pi T_L\partial_t - n_L\partial_\phi)\Big) \\
H_{-1} &= i\Big\{ - (\alpha_1 t + \beta_1\phi)(r-r_+)\partial_r + \frac{\gamma_1}{A(r-r_+)}(\beta_1\partial_t - \alpha_1\partial_\phi) \\
&\quad + \Big((\alpha_1 t + \beta_1\phi)^2 + \frac{\gamma_1^2}{(r-r_+)^2}\Big)\frac{1}{2A}(2\pi T_L\partial_t - 2n_L\partial_\phi)\Big\} \\
\bar{H}_1 &= 2ie^{2\pi T_L\phi - 2n_L t}\Big((r-r_+)\partial_r - \frac{1}{A}(\beta_1\partial_t - \alpha_1\partial_\phi) - \frac{\gamma_1}{A(r-r_+)}(2\pi T_L\partial_r - 2n_L\partial_\phi)\Big) \\
\bar{H}_0 &= i\Big(- \frac{2}{\gamma_1}e^{-2\pi T_L\phi - 2n_L t}(r-r_+)\partial_r - (1 - \frac{2}{\gamma}e^{-2\pi T_L\phi - 2n_L t})\frac{1}{A}(\beta_1\partial_t - \alpha_1\partial_\phi) \\
&\quad + \frac{2e^{-2\pi T_L\phi}}{A(r-r_+)}(2\pi T_L\partial_t - 2n_L\partial_\phi)\Big) \\
\bar{H}_{-1} &= i\Big\{ - \frac{1}{2}\Big(e^{2\pi T_L\phi + 2n_L t} - \frac{4}{\gamma_1^2}e^{-2\pi T_L\phi - 2n_L t}\Big)(r-r_+)\partial_r \\
&\quad - \Big(e^{2\pi T_L\phi + 2n_L t} - \frac{1}{\gamma_1} + \frac{4}{\gamma_1^2}e^{-2\pi T_L\phi - 2n_L t}\Big)\frac{1}{2A}(\beta_1\partial_t - \alpha_1\partial_\phi) \\
&\quad - \Big(e^{2\pi T_L\phi + 2n_L t} + \frac{4}{\gamma_1^2}e^{-2\pi T_L\phi - 2n_L t}\Big)\frac{\gamma_1}{2A(r-r_+)})(2\pi T_L\partial_t - 2n_L\partial_\phi)\Big\}.
\end{aligned} \tag{D.1}
$$

As per 4.3, the quadratic Casimir is then,

$$
\mathcal{H}^2 = \partial_r(\Delta\partial_r) - \Big(\frac{\gamma_1(2\pi T_L\partial_t - 2n_L\partial\phi}{A(r-r_+)}\Big)^2 - \frac{2\gamma_1(2\pi T_L\partial_t - 2n_L\partial\phi)}{(r-r_+)A^2}(\beta_1\partial_t - \alpha_1\partial_\phi), \tag{D.2}
$$

where $A = 2\pi T_L\alpha_1 - 2n_L\beta_1$ and $\Delta = (r-r_+)^2$.

Bibliography

[1] S. W. Hawking and G. F. R. Ellis, *The Large Scale Structure of Space-Time*. Cambridge Monographs on Mathematical Physics. Cambridge University Press, 2011.

[2] A. Dabholkar, "Black hole entropy and attractors," *Class. Quant. Grav.* **23** (2006) S957–S980.

[3] S. M. Carroll, "Lecture notes on general relativity," `arXiv:gr-qc/9712019 [gr-qc]`.

[4] G. Nordström, "On the Energy of the Gravitation field in Einstein's Theory," *Koninklijke Nederlandse Akademie van Wetenschappen Proceedings Series B Physical Sciences* **20** (1918) 1238–1245.

[5] H. Reissner, "Über die Eigengravitation des elektrischen Feldes nach der Einsteinschen Theorie," *Annalen der Physik* **355** no. 9, (1916) 106–120. `https://onlinelibrary.wiley.com/doi/abs/10.1002/andp.19163550905`.

[6] M. Guica, T. Hartman, W. Song, and A. Strominger, "The Kerr/CFT Correspondence," *Phys. Rev.* **D80** (2009) 124008, `arXiv:0809.4266 [hep-th]`.

[7] R. Myers and M. Perry, "Black holes in higher dimensional space-times," *Annals of Physics* **172** no. 2, (1986) 304 – 347. `http://www.sciencedirect.com/science/article/pii/0003491686901867`.

[8] R. Emparan and H. S. Reall, "A Rotating black ring solution in five-dimensions," *Phys. Rev. Lett.* **88** (2002) 101101, `arXiv:hep-th/0110260 [hep-th]`.

[9] H. Elvang, R. Emparan, D. Mateos, and H. S. Reall, "A Supersymmetric black ring," *Phys. Rev. Lett.* **93** (2004) 211302, `arXiv:hep-th/0407065 [hep-th]`.

[10] R. Emparan and H. S. Reall, "Black Holes in Higher Dimensions," *Living Rev. Rel.* **11** (2008) 6, `arXiv:0801.3471 [hep-th]`.

[11] S. W. Hawking, "Particle Creation by Black Holes," *Commun. Math. Phys.* **43** (1975) 199–220. [,167(1975)].

[12] D. A. Lowe and L. Thorlacius, "AdS / CFT and the information paradox," *Phys. Rev.* **D60** (1999) 104012, `arXiv:hep-th/9903237 [hep-th]`.

[13] O. Aharony, S. S. Gubser, J. M. Maldacena, H. Ooguri, and Y. Oz, "Large N field theories, string theory and gravity," *Phys. Rept.* **323** (2000) 183–386, `arXiv:hep-th/9905111 [hep-th]`.

[14] A. Ashtekar, "Gravity and the quantum," *New J. Phys.* **7** (2005) 198, arXiv:gr-qc/0410054 [gr-qc].

[15] M. K. Benna and I. R. Klebanov, "Gauge-String Dualities and Some Applications," *Les Houches* **87** (2008) 611–662, arXiv:0803.1315 [hep-th].

[16] D. Tong, "String Theory," arXiv:0908.0333 [hep-th].

[17] J. Polchinski, *String theory. Vol. 1: An introduction to the bosonic string*. Cambridge Monographs on Mathematical Physics. Cambridge University Press, 2007.

[18] J. D. Brown and M. Henneaux, "Central Charges in the Canonical Realization of Asymptotic Symmetries: An Example from Three-Dimensional Gravity," *Commun. Math. Phys.* **104** (1986) 207–226.

[19] A. Strominger, "Black hole entropy from near horizon microstates," *JHEP* **02** (1998) 009, arXiv:hep-th/9712251 [hep-th].

[20] J. M. Maldacena, "The Large N limit of superconformal field theories and supergravity," *Int. J. Theor. Phys.* **38** (1999) 1113–1133, arXiv:hep-th/9711200 [hep-th]. [Adv. Theor. Math. Phys.2,231(1998)].

[21] E. Witten, "Anti-de Sitter space and holography," *Adv. Theor. Math. Phys.* **2** (1998) 253–291, arXiv:hep-th/9802150 [hep-th].

[22] C. Rovelli, "Loop quantum gravity," *Physics World* .

[23] C. Rovelli, "Loop quantum gravity," *Living Rev. Rel.* **1** (1998) 1, arXiv:gr-qc/9710008 [gr-qc].

[24] S. W. Hawking, G. T. Horowitz, and S. F. Ross, "Entropy, Area, and black hole pairs," *Phys. Rev.* **D51** (1995) 4302–4314, arXiv:gr-qc/9409013 [gr-qc].

[25] R. Wald, *General Relativity*. University of Chicago Press, 1984.

[26] S. W. Hawking, "Black holes and thermodynamics," *Phys. Rev. D* **13** (Jan, 1976) 191–197. https://link.aps.org/doi/10.1103/PhysRevD.13.191.

[27] J. D. Bekenstein, "Black Holes and Entropy," *Phys. Rev. D* **7** (Apr, 1973) 2333–2346. https://link.aps.org/doi/10.1103/PhysRevD.7.2333.

[28] G. Horowitz, *Black Holes in Higher Dimensions*. Cambridge University Press, 2012. https://books.google.co.za/books?id=5pGzAQAACAAJ.

[29] P. Di Francesco, P. Mathieu, and D. Senechal, *Conformal Field Theory*. Graduate Texts in Contemporary Physics. Springer-Verlag, New York, 1997. http://www-spires.fnal.gov/spires/find/books/www?cl=QC174.52.C66D5::1997.

[30] H. Nastase, "Introduction to AdS-CFT," arXiv:0712.0689 [hep-th].

[31] J. L. Petersen, "Introduction to the Maldacena conjecture on AdS / CFT," *Int. J. Mod. Phys.* **A14** (1999) 3597–3672, arXiv:hep-th/9902131 [hep-th].

[32] J. M. Bardeen and G. T. Horowitz, "The Extreme Kerr throat geometry: A Vacuum analog of AdS(2) x S**2," *Phys. Rev.* **D60** (1999) 104030, arXiv:hep-th/9905099 [hep-th].

[33] M. Guica, "Asymptotic symmetries, black holes, and holography - IphT Lecture Notes," (2018) .

[34] V. Balasubramanian, J. de Boer, M. M. Sheikh-Jabbari, and J. Simon, "What is a chiral 2d CFT? And what does it have to do with extremal black holes?," *JHEP* **02** (2010) 017, arXiv:0906.3272 [hep-th].

[35] G. Compère, "The Kerr/CFT correspondence and its extensions," *Living Rev. Rel.* **15** (2012) 11, arXiv:1203.3561 [hep-th]. [Living Rev. Rel.20,no.1,1(2017)].

[36] G. Compère and A. Fiorucci, "Advanced Lectures on General Relativity," arXiv:1801.07064 [hep-th].

[37] I. Bredberg, C. Keeler, V. Lysov, and A. Strominger, "Cargese Lectures on the Kerr/CFT Correspondence," *Nucl. Phys. Proc. Suppl.* **216** (2011) 194–210, arXiv:1103.2355 [hep-th].

[38] E. P. Verlinde, "On the holographic principle in a radiation dominated universe," arXiv:hep-th/0008140 [hep-th].

[39] S. Carlip, "Extremal and nonextremal Kerr/CFT correspondences," *JHEP* **04** (2011) 076, arXiv:1101.5136 [gr-qc]. [Erratum: JHEP01,008(2012)].

[40] T. Hartman, C. A. Keller, and B. Stoica, "Universal Spectrum of 2d Conformal Field Theory in the Large c Limit," *JHEP* **09** (2014) 118, arXiv:1405.5137 [hep-th].

[41] O. Coussaert and M. Henneaux, "Selfdual solutions of (2+1) Einstein gravity with a negative cosmological constant," arXiv:hep-th/9407181 [hep-th]. [,25(1994)].

[42] A. Castro, A. Maloney, and A. Strominger, "Hidden Conformal Symmetry of the Kerr Black Hole," *Phys. Rev.* **D82** (2010) 024008, arXiv:1004.0996 [hep-th].

[43] R. Emparan and H. S. Reall, "Black Rings," *Class. Quant. Grav.* **23** (2006) R169, arXiv:hep-th/0608012 [hep-th].

[44] H. Elvang, "A Charged rotating black ring," *Phys. Rev.* **D68** (2003) 124016, arXiv:hep-th/0305247 [hep-th].

[45] A. A. Pomeransky and R. A. Sen'kov, "Black ring with two angular momenta," arXiv:hep-th/0612005 [hep-th].

[46] R. Emparan and H. S. Reall, "A Rotating black ring solution in five-dimensions," *Phys. Rev. Lett.* **88** (2002) 101101, arXiv:hep-th/0110260 [hep-th].

[47] B. Chen and J.-j. Zhang, "Holographic Descriptions of Black Rings," *JHEP* **11** (2012) 022, arXiv:1208.4413 [hep-th].

[48] P. Moon and P. Spencer, *Field Theory Handbook*. Springer-Verlag, 1971.

[49] C. Keeler and F. Larsen, "Separability of Black Holes in String Theory," *JHEP* **10** (2012) 152, `arXiv:1207.5928 [hep-th]`.

[50] V. P. Frolov and D. Kubiznak, "Higher-Dimensional Black Holes: Hidden Symmetries and Separation of Variables," *Class. Quant. Grav.* **25** (2008) 154005, `arXiv:0802.0322 [hep-th]`.

[51] H. Elvang, R. Emparan, D. Mateos, and H. S. Reall, "Supersymmetric black rings and three-charge supertubes," *Phys. Rev.* **D71** (2005) 024033, `arXiv:hep-th/0408120 [hep-th]`.

[52] K. Goldstein and R. P. Jena, "One entropy function to rule them all..." *JHEP* **11** (2007) 049, `arXiv:hep-th/0701221 [hep-th]`.

[53] F. Loran and H. Soltanpanahi, "Near the horizon of 5D black rings," *JHEP* **03** (2009) 035, `arXiv:0810.2620 [hep-th]`.

[54] H. Golchin, M. M. Sheikh-Jabbari, and A. Ghodsi, "Dual 2d CFT Identification of Extremal Black Rings from Holes," *JHEP* **10** (2013) 194, `arXiv:1308.1478 [hep-th]`.

[55] B. Chen, J. Long, and J.-j. Zhang, "Hidden Conformal Symmetry of Extremal Black Holes," *Phys. Rev.* **D82** (2010) 104017, `arXiv:1007.4269 [hep-th]`.

[56] B. Chen and J.-j. Zhang, "General Hidden Conformal Symmetry of 4D Kerr-Newman and 5D Kerr Black Holes," *JHEP* **08** (2011) 114, `arXiv:1107.0543 [hep-th]`.

[57] M. Cyrier, M. Guica, D. Mateos, and A. Strominger, "Microscopic entropy of the black ring," *Phys. Rev. Lett.* **94** (2005) 191601, `arXiv:hep-th/0411187 [hep-th]`.

[58] F. Loran and H. Soltanpanahi, "5D Extremal Rotating Black Holes and CFT duals," *Class. Quant. Grav.* **26** (2009) 155019, `arXiv:0901.1595 [hep-th]`.

[59] A. Castro, J. M. Lapan, A. Maloney, and M. J. Rodriguez, "Black Hole Monodromy and Conformal Field Theory," *Phys. Rev.* **D88** (2013) 044003, `arXiv:1303.0759 [hep-th]`.

[60] A. Castro, J. M. Lapan, A. Maloney, and M. J. Rodriguez, "Black Hole Scattering from Monodromy," *Class. Quant. Grav.* **30** (2013) 165005, `arXiv:1304.3781 [hep-th]`.

[61] A. Castro, "Black Hole Monodromy and CFT," *Unpublished Work* (2012) .

[62] M. Rogatko, "Uniqueness theorem for stationary black ring solution of sigma-models in five dimensions," *Phys. Rev.* **D77** (2008) 124037, `arXiv:0805.1982 [hep-th]`.

[63] S. Tomizawa, Y. Yasui, and A. Ishibashi, "Uniqueness theorem for charged dipole rings in five-dimensional minimal supergravity," *Phys. Rev.* **D81** (2010) 084037, `arXiv:0911.4309 [hep-th]`.

[64] V. Kisil, "Starting with the group SL2(R),".

[65] V. Kisil, “Poincare Extension of Moebius Transformations,” *arXiv e-prints* (Jul, 2015) arXiv:1507.02257, arXiv:1507.02257 [math.CV].

[66] B. C. Hall, *Lie groups, Lie algebras, and representations. An elementary introduction*. 01, 2003.

[67] C. R. Schneider, “SL(2,R) Actions on Surfaces,” *American Journal of Mathematics* **96** no. 4, (1974) 511–528. http://www.jstor.org/stable/2373705.

[68] S. Lang, *SL2(R)*. Graduate Text in Mathematics. Springer, 1985.

[69] O. Coussaert and M. Henneaux, “Selfdual solutions of (2+1) Einstein gravity with a negative cosmological constant,” arXiv:hep-th/9407181 [hep-th]. [,25(1994)].